Radiative effects in scattering of polarized leptons by polarized nucleons and light nuclei

I. Akushevich[a)]*, A.Ilyichev[b)], N.Shumeiko[b)]

[(a)] *North Carolina Central University, Durham, NC 27707, USA*
and
Jefferson Lab, Newport News, VA 23606, USA
[(b)] *National Center of Particle and High Energy Physics, 220040 Minsk, Belarus*

Abstract

Recent developments in the field of radiative effects in polarized lepton-nuclear scattering are reviewed. The processes of inclusive, semi-inclusive, diffractive and elastic scattering are considered. The explicit formulae obtained within the covariant approach are discussed. FORTRAN codes POLRAD, RADGEN, HAPRAD, DIFFRAD and MASCARAD created on the basis of the formulae are briefly described. Applications for data analysis of the current experiments on lepton-nuclear scattering at CERN, DESY, SLAC and TJNAF are illustrated by numerical results.

*on leave of absence from the National Center of Particle and High Energy Physics, 220040 Minsk, Belarus

Contents

Introduction

Starting with the late nineteen sixties the main source of information about internal nature of nucleon is lepton nuclei scattering. Nowadays experimental design of modern detectors opens possibility for large set of experimental data during short period of time. As a result the calculation of background radiative effects or the procedure of radiative corrections (RC) is a quite important thing.

While considering lepton nucleon scattering it should be noted that the main contribution to the observables gives subprocess with one photon exchange graphs that is called Born process. However all sets of experimental data consist of not only such contribution, but of other processes appearing during the measurement which are called background ones because of their small contributions to the observables. Therefore the main task of data processing in experiments on lepton nucleon scattering is the extraction of the one-photon exchange contribution. It leads to the necessity to cancel the background events from all data sets. When it cannot be made by experimental methods the correspond contributions can be calculated in the frame of some theory. Usually a such kind of contribution depends on the quantities (the structure function, asymmetries), that are observables in the given experiment. As a result we come to the necessity of the iteration procedure application for the extraction of the observables on Born level from the full set of experimental data. This procedure is usually called as the procedure of RC of experimental data.

There are two basic methods of calculation of model independent QED radiative correction. First one is connected with introducing of an artificial parameter separating the

momentum phase space into soft and hard parts. One can find a classical review introducing this formalism in ref. [1, 2]. However the presence of the artificial parameter is a disadvantage of this method. For the soft photon part the calculation is performed in such approximation when the photon energy is considered to be small with respect to all momenta and masses in the problem. So this parameter should be chosen as small as possible to reduce the region evaluated approximately. From the other side it cannot be chosen too small because of possible numerical instabilities in calculating of hard-photon emission. Calculation within the approach of Mo and Tsai was performed only for the case of unpolarized deep inelastic scattering. In the end of seventies Bardin and Shumeiko developed an approach [3] of extraction and cancellation of infrared divergence without introducing this artificial parameter. Then this approach was applied to the calculation of electromagnetic correction to the lepton current for deep inelastic scattering (DIS) [4–12] as well as for some approximation and taking into account the contribution of net soft photon emission. The exact expressions for the lowest order QED RC to polarized DIS of polarized leptons by polarized light nuclei including targets of spin 1 such as deuterium are presented in [13]. Basing on these formulae FORTRAN code POLRAD [14] are constructed. Besides, some others tasks such as Monte Carlo generator RADGEN [15] was made, RC both to diffractive vector meson electroproduction [16, 17] and to spin-density matrix elements in the exclusive vector meson production [18] by this method were solved. Recently Bardin-Shumeiko approach has being applied to experiment on polarized elastic electron-proton scattering at TJNAF [19, 20]. The comprehensive analysis of some results obtained by [1, 2] and [3] was made in [15, 21].

The formulae of [3] as well as [22] allow along with using the parton model to estimate the value of electromagnetic correction to the hadronic current in unpolarized [23] and polarized [24, 25] lepton nucleon DIS.

Other important source of contributions to systematic error of experiments with high energy scattering particles together with electromagnetic effects is electroweak ones. When the square transferred momentum is high enough the contribution of Z-boson change is compared with electromagnetic one especially on the kinematic borders. Therefore it is useful to have the calculation of RC within the standard model of electroweak interactions. This task is especially actual for experiments at collider [26, 27]. This calculation requires choosing renormalization scheme and fixation the gauge. Detailed description of on-mass scheme within t'Hooft Feynman gauge were reviewed in [28, 29].

The calculation of electroweak corrections to the lepton legs for DIS could be found in [30–32]. Electroweak corrections to the hadronic current in quark-partonic model (QMP) can be found in [33–36] and [37] for unpolarized and polarized DIS respectively.

The calculation of RC within the structure function method was suggest by Kuraev and Fadin [38] and applied for DIS [39]. This method was used for the calculation of Compton tensor with heavy photon in the case of unpolarized [40] and longitudinal-polarized [41] fermions. The calculation of LO and NLO corrections to radiative tail from elastic peak in DIS can be found in [42].

The next step is the calculation of higher level RC $\sim \alpha^2$. Notice that such kind of correction to the elastic tail was calculated in [5, 42]. As to the continuous spectrum the obtaining of the formulae not only in exact form (like [13]) but and in ultrarelativistic approximation is a quite difficult task (first of all because of the problem of the integration over the photon emission phase space). Therefore we consider the correction $\sim \alpha^2$ to the continuous spectrum in the LO approximation. For unpolarized particles such correction

in LO and NLO approximation was found in [38, 43].

Another important source of radiative effects in DIS is QCD-correction appearing from gluon emission. However QCD corrections, in spite of photon emission is not extracted from the structures functions but is directly included into their definition. As a result the structure functions start depending not only on a scaling variable x but on the transferred momentum squared.

A lot of articles dedicated to NLO QCD corrections to polarized DIS have been published. The calculations in most of them are performed in the assumption that the quark mass is equal to zero (see review [54] and reference there). However there are some works when the authors estimate a finite quark mass effect for both unpolarized [46] and polarized structure functions [47–53]. The main difference of these two approaches is the method of tending the quark mass to zero and the procedure of integration of the squared matrix element over the phase space of an emitted gluon. In the massless approach a fermion mass is equal to zero *before* the integration while in the massive one this quantity goes to zero *after* the integration and survives only in LO terms.

Notice that QCD and QED radiative corrections (RC) having different origins possess some common features on the one-loop level. If our consideration is restricted to so-called QCD Compton process then both corrections should be described by the identical sets of Feynman graphs. The transition from the strong radiative effects to the electromagnetic ones could be performed by the following replacement:

$$\frac{4}{3}\alpha_s \to e_q^2\alpha_{QED}. \tag{1}$$

Due to these facts in [54] the mentioned above Bardin Shumeiko method was applied to the investigation of Compton effects within QCD. This calculation is actual because it allows us to estimate the influence of the finite quark mass on observables in DIS like it was done in [46–51].

In the present poster which is basing on ref. [7, 11, 13–20, 32, 44, 54] some radiative effects in polarized lepton by polarized light nuclei scattering is reviewed. In the first and last sections the lowest order corrections are calculated within Bardin Shumeiko approach as well as the next order correction for leptonic current are estimated in the leading level by the method described in [43]. The calculation of QCD-correction to the hadronic current is reviewed with [54].

1 Corrections to the lepton current in DIS

1.1 Inclusive physics

Let us consider the process of polarized lepton-nucleon DIS

$$l(k_1, \xi) + N(p, \eta) \to l'(k_2) + X \tag{2}$$

where k_1, p (ξ, η) are the momenta (polarization vectors) of the initial particles, k_2 is the final lepton momentum and X is a final hadronic state.

At the Born or one photon exchange level (fig.1a) the cross section of the considered process can be presented by the convolution of the leptonic tensor $L_{\mu\nu}$ having well known

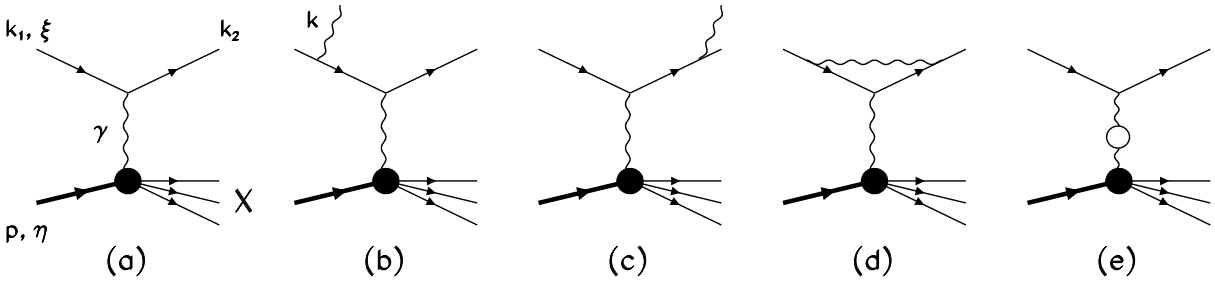

Figure 1: *Feynman diagrams contributing to the Born and the model independent QED correction of the lowest order. The letters denote the four-momenta and polarizations of corresponding particles.*

structure, with the hadronic one $W_{\mu\nu}$. The latter can be expanded into Lorentz covariants whose coefficients define the structure function which are to be measured.

As a result the double differential Born cross section has the form [1]

$$\begin{aligned}\sigma_0 &= \frac{4\pi\alpha^2}{\lambda_s}\frac{SS_x}{Q^4}\Big\{(Q^2-2m^2)\Im_1+(SX-M^2Q^2)\frac{\Im_2}{2M^2}\\ &+mMP_L\left(2(Q^2\,\xi\eta-q\eta\;k_2\xi)\frac{\Im_3}{M^2}+(S_x\;k_2\xi-2\;\xi p\;Q^2)q\eta\frac{\Im_4}{M^4}\right)\\ &+(Q^2-2m^2)(Q^2-3(q\eta)^2)\frac{\Im_5}{M^2}+(SX-M^2Q^2)(Q^2-3(q\eta)^2)\frac{\Im_6}{2M^4}\\ &-\frac{1}{2}\,(\,Q^2+4m^2+12\;\eta k_1\;\eta k_2\,)\,\Im_7-\frac{3}{2}(X\;\eta k_1+S\;\eta k_2)q\eta\frac{\Im_8}{M^2}\Big\},\end{aligned} \tag{3}$$

where the kinematic invariants defined in the standard way:

$$\begin{gathered}S=2k_1p,\;X=2k_2p=(1-y)S,\;Q^2=-q^2=-(k_1-k_2)^2=xyS,\\ S_x=S-X,\;S_p=S+X,\;\lambda_s=S^2-4m^2M^2,\end{gathered} \tag{4}$$

and $x=Q^2/S_x$, $y=S_x/S$ are usual scaling variables. The explicit expression for the hadronic tensor and the generalized structure functions $\Im_i$ can be found in Appendix A.1 of [14].

Now and later we deal with both longitudinal and transversal polarized targets. At the same time the initial lepton will be polarized longitudinally and its polarization vector can be presented as the sum of two parts:

$$\xi=\frac{S}{m\sqrt{\lambda_s}}k_1-\frac{2m}{\sqrt{\lambda_s}}p=\xi_0+\xi_1. \tag{5}$$

Notice, that in ultrarelativistic approximation over the lepton mass a non-zero contribution to the polarized part of cross section (3) appears from ξ_0 as well as the second part

[1] Now and later $\sigma\equiv d^2\sigma/dxdy$.

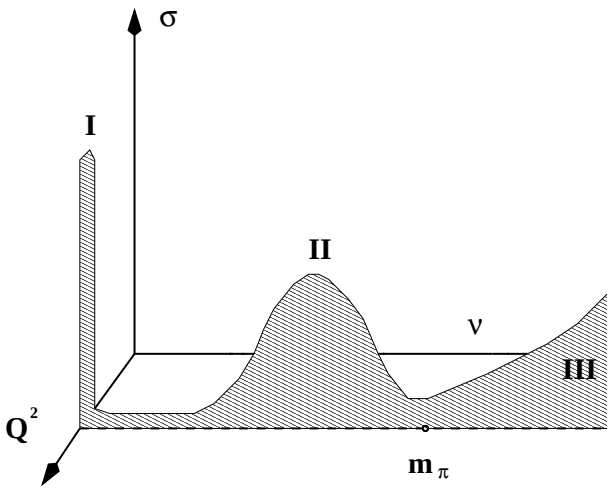

Figure 2: *The double differential cross section for inclusive lepton-nuclei scattering sketched at a certain value of Q^2 as function of ν (arbitrary scale). The three basic channels are the elastic (I), the quasielastic (II), and the inelastic (III) one.*

of polarization vector ξ_1 gives a non zero contribution to the cross section of DIS within $m \to 0$ by the correction from real photon emission.

The natural approximation for high energies of the scattering particles is ultrarelativistic one

$$m^2, M^2 \ll S, X, Q^2. \tag{6}$$

Within this approximation the Born cross section has the form

$$\sigma_0^{||} = \frac{4\pi\alpha^2 S}{Q^4}((F_1 - \frac{Q_N}{3}b_1)xy^2 + (F_2 - \frac{Q_N}{3}b_2)(1-y) - P_L P_N xy(2-y)g_1) \tag{7}$$

for longitudinal polarized nucleus and

$$\begin{aligned}\sigma_0^{\perp} = \quad & \frac{4\pi\alpha^2 S}{Q^4}((F_1 + \frac{Q_N}{6}b_1)xy^2 + (F_2 + \frac{Q_N}{6}b_2)(1-y) \\ & -2P_L P_N \frac{x\sqrt{xy(1-y)}M}{\sqrt{S}}(yg_1 + 2g_2))\end{aligned} \tag{8}$$

for transversal polarized one.

It is well-known that there are three scattering channels of virtual boson (γ, Z) on nucleus in dependence on the transfer energy $\nu = E_1 - E_2$, where $E_1(E_2)$ is the initial (scattered) lepton energy: elastic, quasielastic and inelastic. Representative plot of dependence of the scattering cross section on ν and square of transfer momentum $Q^2 = -q^2$ is shown on fig.1 (only for the regions that give sufficient contribution to RC calculation). the peak in the range I (for $\nu = 0$, when neglecting nuclear recoil) corresponds to the elastic scattering. Then the nucleus remains in the ground state. Range II stands for the quasielastic scattering i.e. direct collisions of leptons with nucleons inside nucleus. A wide maximum in the energy spectrum originates from the own movement of nucleons. Range III of inelastic scattering occurs when the transfer energy is greater then pion threshold.

On the Born level both ν and Q^2 are fixed by the measurements of the scattered photon momentum. Hence, the channel of scattering is fixed too. However, on a level of

RC radiated real photon momentum is indefinite, and ν and Q^2 are arbitrary so each of three channels contributes to cross section. Integration over the photon phase space may be presented in the plane of ν and Q^2. Adding the virtual photon contribution σ^v, we have for the RC cross section

$$\sigma_{RC} = \sigma^{in} + \sigma^{el} + \sigma^q + \sigma^v. \tag{9}$$

Here σ^{in}, σ^{el}, σ^q are contributions of radiative tails from continuous spectrum, of the elastic scattering radiative tail, of the radiative tail from the quasielastic scattering respectively. Also the contribution of electroweak correction calculated in the quark-parton model is contained in σ^{in}. Both α and α^2 corrections are taken into account in $\sigma^{in,el,q,v}$. To separate the contributions we introduce the lower index, f.e. $\sigma^{in} = \sigma_1^{in} + \sigma_2^{in}$.

A modern approach of solving the task on RC calculation assumes exact calculation of the lowest order model independent correction. This correction includes the QED processes of radiation of unobserved real photon and one-loop diagrams to lepton line. These processes gives the largest contribution, which can be calculated exactly. Uncertainties of the model independent RC can come only from fits and models used for the structure functions. The calculation of model dependent correction (box-type diagrams, emission by hadrons) requires additional assumptions about hadron interaction, so it has additional pure theoretical uncertainties, which are hardly controlled. The model-dependent correction is much smaller compared to leptonic radiation because it does not include a large logarithmic term $\log(Q^2/m^2)$. In this and last sections we concentrate on the calculation of model independent correction as main contribution to total RC.

The explicit expression for the lowest-order QED correction (see fig.1b-e) can be found in [13]. Thus, for infrared free sum σ_1^{in} (fig.1(a,b)) and σ_1^v (fig.1(c,d)) we have

$$\sigma_1^v + \sigma_1^{in} = \frac{\alpha}{\pi}\delta_v\sigma_o + \sigma_F^{in}. = \frac{\alpha}{\pi}(\delta_R^{IR} + \delta_{vert} + \delta_{vac}^l + \delta_{vac}^h)\sigma_o + \sigma_F^{in}. \tag{10}$$

The finite contribution from real photon emission

$$l(k_1,\xi) + N(p,\eta) \to l'(k_2) + \gamma(k) + X \tag{11}$$

can be presented in a following way:

$$\sigma_F^{in} = -\alpha^3 y \int\limits_{\tau_{min}}^{\tau_{max}} d\tau \sum_{i=1}^{8} \left\{ \theta_{i1}(\tau) \int\limits_0^{R_{max}} \frac{dR}{R} \left[\frac{\Im_i(R,\tau)}{(Q^2+R\tau)^2} - \frac{\Im_i(0,0)}{Q^4} \right] + \sum_{j=2}^{k_i} \theta_{ij}(\tau) \int\limits_0^{R_{max}} dR \frac{R^{j-2}}{(Q^2+R\tau)^2} \Im_i(R,\tau) \right\}, \tag{12}$$

where

$$R = 2kp, \quad \tau = kq/kp \tag{13}$$

and k is a momentum of emission photon ($k^2 = 0$). The limits of integration are defined as

$$R_{max} = \frac{W^2 - (M+m_\pi)^2}{1+\tau}, \quad \tau_{max,min} = \frac{S_x \pm \sqrt{\lambda_Q}}{2M^2},$$
$$\lambda_Q = S_x^2 + 4M^2Q^2, \quad W^2 = S_x - Q^2 + M^2, \tag{14}$$

where m_π is a pion mass. The explicit expression for functions $\theta_{ij}(\tau)$ are presented in [13, 14].

The quantity δ_R^{IR} appears when the infrared divergence is extracted in accordance with the Bardin and Shumeiko method [3] from σ^{in}. The virtual photon contribution consists of the lepton vertex correction δ_{vert} (fig.1(d)) and the vacuum polarization (fig.1(e)) by leptons δ_{vac}^l and by hadrons δ_{vac}^h [55]. These corrections are given by formulae (20-25) of ref. [13].

In the case of elastic scattering the nucleus remains in the ground state, so for the integration variable R we have an additional relation

$$R = R_{el} = (S_{xA} - Q^2)/(1 + \tau_A), \tag{15}$$

resulting in

$$\sigma_1^{el} = \frac{1}{A}\frac{d^2\sigma^{el}}{dx_A dy} = -\frac{\alpha^3 y}{A^2}\int\limits_{\tau_{Amin}}^{\tau_{Amax}} d\tau_A \sum_{i=1}^{8}\sum_{j=1}^{k_i}\theta_{ij}(\tau_A)\frac{2M_A^2 R_{el}^{j-2}}{(1+\tau_A)(Q^2+R_{el}\tau_A)^2}\Im_i^{el}(R_{el},\tau_A). \tag{16}$$

Here invariants with the index "A" contain the nucleus momentum p_A instead of p ($p_A^2 = M_A^2$, M_A is nucleus mass). The quantities $\Im_i^{el}$ are given in Appendix 1 of [14].

Quasielastic scattering corresponds to direct collisions of leptons with nucleons inside nucleus. Due to self movement of nucleons we have no additional relation like (15). As a result we have to integrate numerically both over R and τ

$$\sigma_1^q = -\frac{\alpha^3 y}{A}\int\limits_{\tau_{min}}^{\tau_{max}} d\tau \sum_{i=1}^{8}\sum_{j=1}^{k_i}\theta_{ij}(\tau)\int\limits_{R_{min}^q}^{R_{max}^q} dR\frac{R^{j-2}}{(Q^2+R\tau)^2}\Im_i^q(R,\tau). \tag{17}$$

The quantities $\Im_i^q$ can be obtained in the terms of quasielastic structure functions (so-called response functions, see [14] for explicit result), which have a form of the peak for $\omega = Q^2/2M$. Due to the absence of enough experimental data the fact is normally used for construction of the peak type approximation. The factors at response functions are estimated at the peak, and subsequent integration of response functions leads to results in terms of suppression factors $S_{E,M,EM}$ (or of sum rules for electron-nucleus scattering [56]):

$$\sigma_1^q = -\frac{\alpha^3 y}{A}\int\limits_{\tau_{min}}^{\tau_{max}} d\tau \sum_{i=1}^{4}\sum_{j=1}^{k_i}\theta_{ij}(\tau)\frac{2M^2 R_q^{j-2}}{(1+\tau)(Q^2+R\tau)^2}\Im_i^q(R_q,\tau). \tag{18}$$

Detailed comparison of the results for quasielastic tail obtained within different approaches can be found in [9].

To take into account the effect of radiation of many soft photons a special procedure of exponentiation was applied [12]. It can be realized by the following substitutions:

$$\begin{gathered}\sigma_1^{el} \to \left(\frac{y^2(1-x/A)^2}{1-xy/A}\right)^{t_r}\sigma_1^{el}, \qquad \sigma_1^q \to \left(\frac{y^2(1-x)^2}{1-xy}\right)^{t_r}\sigma_1^q, \\ (1+\frac{\alpha}{\pi}\delta_v)\sigma_o \to \exp\left(\frac{\alpha}{\pi}\delta_{inf}\right)(1+\frac{\alpha}{\pi}(\delta_v-\delta_{inf}))\sigma_o,\end{gathered} \tag{19}$$

where $t_r = \dfrac{\alpha}{\pi}(l_m - 1)$.

1.2 Iteration procedure of data processing

In this subsection the procedure of radiative correction to extract the structure function $g_1(x)$ from measured spin asymmetry A_{1i}^m is considered. The spin average structure functions are considered to be constant and $g_2(x)$ equals to 0. The measured asymmetry is defined as

$$A_1^m = \frac{g_1}{F_1} + \Delta A_1(g_1), \tag{20}$$

where the radiative correction to asymmetry ΔA_1 can be written in terms of spin-average and spin-dependent parts ($\sigma^{u,p}$) of cross sections (9)

$$\Delta A_1 = \frac{\sigma_0^u(\sigma_p^{in}(g_1) + \sigma_p^q + \sigma_p^{el}) - \sigma_0^p(g_1)(\sigma_u^{in} + \sigma_u^q + \sigma_u^{el})}{\sigma_0^u((1+\delta_v)\sigma_0^u + \sigma_u^{in} + \sigma_u^q + \sigma_u^{el})}, \tag{21}$$

where $\delta_v = \sigma_p^v/\sigma_0^p = \sigma_u^v/\sigma_0^u$. The Born and inelastic radiative tail polarized parts of cross sections depend on SF g_1, and in the last case the dependence is non-trivial. So the equation (20) becomes functional one in g_1. This functional equation transforms into a system considering the extraction of g_1 in concrete binning over x in n kinematic points x_i $(i = 1, ..., n)$:

$$A_{1i}^m = \frac{g_{1i}}{F_1} + \Delta A_1(g_{1j}; j = 1, ..., n). \tag{22}$$

Usually the iteration methods are used to solve such a system of equations. The variant of iteration formula is ambiguous, but in practice only two types are used. The first and most evident one is to take for k-th step:

$$g_{1i}^{(k)} = F_1(A_{1i}^m - \Delta A_1(g_{1j}^{(k-1)}; j = 1, ..., n)). \tag{23}$$

Another possibility to obtain the formulae for iteration procedure arises when both Born and radiative correction cross section are separated into spin-averaged and spin-dependent parts. Then for the measured asymmetry we have

$$A_1^m = \frac{1}{D}\frac{\sigma_0^p + \sigma_1^p}{\sigma_0^u + \sigma_1^u} = \frac{g_1/F_1 + \sigma_1^p/D\sigma_0^u}{1 + \sigma_1^u/\sigma_0^u}. \tag{24}$$

Thus we obtain the iteration formulae

$$g_{1i}^{(k)} = F_1\left[A_{1i}^m\left(1 + \frac{\sigma_1^u}{\sigma_0^u}\right) - \frac{\sigma_1^p(g_{1j}^{(k-1)}; j = 1, ..., n)}{D\sigma_0^u}\right], \tag{25}$$

where in right-hand side the dependence on g_1 is contained only on the level of RC, but not on the Born level.

The above presented formulae could be applied directly for experimental data on hydrogen and deuteron. Three-parameter fit is used for fitting of the spin asymmetry [57–60]:

$$\begin{aligned} A_1^p(x) &= A + x^B(1 - e^{-Cx}), \\ A_1^d(x) &= (e^{-Ax} - 1)(B^C - x^C). \end{aligned} \tag{26}$$

For proton asymmetry the one- and two parameter fits are also used:

$$A_1^p(x) = x^B, \qquad A_1^p(x) = Ax^B. \tag{27}$$

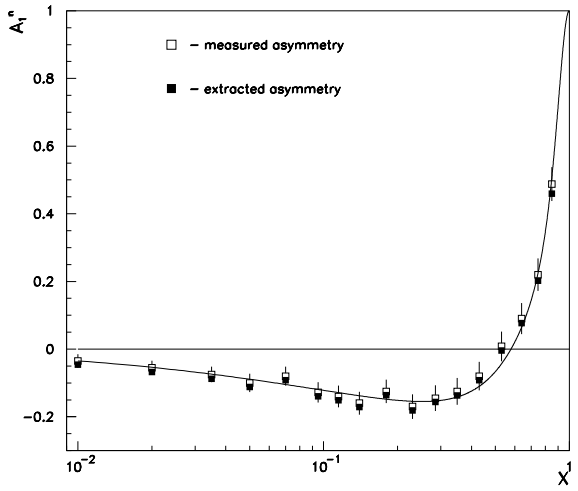

Figure 3: *The results of iteration procedure for spin asymmetry along with the fit constructed.*

For the neutron asymmetry extracted from the deuteron and helium-3 data the nuclear corrections have to be taken into account:

$$A_1^n(x) = \frac{A_1^{D,^3\mathrm{He}}(x) - (1 - f_d(x))P_p A_1^p(x)}{f_d(x)P_n}. \tag{28}$$

Dilution factors for both cases are given by the formulae

$$f_d(x) = \frac{1}{F_2^p/F_2^n + 1}, \qquad f_d(x) = \frac{1}{2F_2^p/F_2^n + 1} \tag{29}$$

respectively. The numbers P_p and P_n are effective nucleon polarizations in nucleus. For deuteron target $P_p = P_n = 0.5 - 0.75\omega_d$, where ω_d is the D-state probability ($\sim$5%), and P_p=-0.028 and P_n=0.86 for helium-3.

The application of procedure of RC for experiments on DIS with polarized ^{3}He and HERMES lepton beam with energies $E = 27.5$ GeV on fig.3 are demonstrated.

Another important question carefully studied in all experiments on lepton-nucleon scattering is contribution to systematical error of measurement due to radiative corrections. There are several sources for this uncertainty: the RC procedure itself, dependence on SF models beyond measured region and physical processes neglected in the standard RC procedure. Monte Carlo approach for estimations of these effects is presented in [61] for the case of ^{3}He polarized target.

1.3 Semi-inclusive physics

We calculate the radiative corrections to data of semi-inclusive polarized experiments

$$e(k_1) + N(p) \longrightarrow e'(k_2) + h(p_h) + X(p_x) \tag{30}$$

when a hadron h is detected in coincidence with the outgoing lepton. In this case the cross section depends on five kinematic variables which can be chosen as

$$x,\ y;\ z,\ t,\ \phi_h, \tag{31}$$

where x and y are usual scaling variables, z and t are defined via hadron momentum

$$t = (q - p_h)^2, \quad z = p_h p/pq, \quad q = k_1 - k_2, \tag{32}$$

ϕ_h is an angle between planes $(\vec{k}_1, \vec{k}_2)$ and $(\vec{q}, \vec{p}_h)$ in the rest frame ($p = (M, \vec{0})$). Instead of $t-$dependence we will also consider the cross section as a function of transversal momentum p_t defined in (A.8) of [11]. Also the following invariants will be used

$$M_x^2 = p_x^2 = (1 - z)S_x + M^2 + t, \; V_{1,2} = 2k_{1,2}p_h. \tag{33}$$

Notice that there are two tasks for this process. The first task corresponds the description of semi-inclusive DIS in the frame of quark-parton model. In this way the cross section depends on three variables x, y and z. However for the real situation the integration region is limited by the experimental cuts. To deal with them on the angles of registered hadron a special procedure was developed and cross section describing such situation is defined by five variables: three standard x, y, z and two additional p_t, ϕ_h. The relation between these two cross sections can be established as follows:

$$\frac{d\sigma_R}{dxdydz} = \int \frac{1}{2\pi}\frac{d^3k}{2k_0}\frac{d\tilde{z}}{dz} dp_t d\phi_h \theta(\sin^2\vartheta_{max} - \sin^2\vartheta)\theta(\sin^2\vartheta - \sin^2\vartheta_{min}) \frac{d\sigma}{dxdydzdp_t d\phi_H}, \tag{34}$$

if θ-function are removed. Here ϑ is the angle between the beam direction $(\vec{k}_1)$ and hadron momentum in the lab frame.

Within quark-parton model for the Born cross section of longitudinal polarized semi-inclusive DIS we have

$$\sigma_0^s \equiv \frac{d^3\sigma_0}{dxdydz} = \frac{2\pi\alpha^2}{Sxy}[F_0^u \Sigma^+(x,z) + P_L P_N F_0^p \Sigma^-(x,z)] \tag{35}$$

where

$$F_0^u = 2(1/y - 1 - \mu_N x) + y, \qquad F_0^p = y - 2, \qquad \mu_N = M^2/S. \tag{36}$$

The quantities

$$\Sigma^{+(-)}(x,z) = \sum_q e_q^2 [f_q^+(x) \pm f_q^-(x)] D_q^H(z) \tag{37}$$

is the ordinary for QPM combination of the distribution functions $f_q^{+(-)}(x)$ for the quark of flower q polarized (anti)parallel to the nucleon polarization, and of the fragmentation functions $D_q^h(z)$ of the quark q into the hadron h, e_q being the quark charge in units of elementary charge.

As it was mentioned above there are three radiative tails give contribution to DIS:inelastic, elastic and quasielastic (see Fig 2). However, in semi-inclusive process the transfer energy is above pion threshold, so in RC calculation one have to take into account only σ^{in} and σ^v. The lowest order QED correction was calculated in ref. [7] and presented in [14] as the sum of factorizing and non-factorizing infrared free parts

$$\sigma_{EM} \equiv \frac{d^3\sigma_{EM}}{dxdydz} = \frac{\alpha}{\pi}\delta_{VR}\sigma_0^s + \sigma_R^F, \tag{38}$$

where the first one is the sum of infrared divergence separated from radiative tail and the additional virtual photon contribution: $\delta_{VR} = \delta_V + \delta_R^{IR}$.

The finite part of (35) has the form

$$\sigma_R^F = \frac{2\alpha^3}{S}\int\limits_{t_{1d}}^{t_{1u}} dt_1 \int\limits_{t_{2d}}^{t_{2u}} dt_2 \{\frac{y^2}{x_t^2 y_t}[F_R^u \Sigma^+(\tilde{x},\tilde{z}) + P_L P_N F_R^p \Sigma^-(\tilde{x},\tilde{z})] - \\ -\frac{\theta(t_{1i}-t_1)}{xy}[F_{IR}^u \Sigma^+(x,z) + P_L P_N F_{IR}^p \Sigma^-(x,z)]\}, \tag{39}$$

The definition of the rest quantities can be found in [14]

In order to write five-dimensional cross section it is useful to take the some scalar products with p_h in the form

$$\frac{1}{2}V_{1,2} = k_{1,2}p_h = a^{1,2} + b\cos\phi_h \tag{40}$$
$$\frac{1}{2}\mu R = kp_h = R(a^k + b^k(\cos\phi_h\cos\phi_k + \sin\phi_h\sin\phi_k)).$$

where $\mu = kp_h/kp$ and ϕ_k is the rest frame angle between planes $(\vec{k}_1, \vec{k}_2)$ and $(\vec{q}, \vec{k})$. We will use $a^{\pm} = a^2 \pm a^1$. The explicit expressions for coefficients are given in [11].

As a result the five-dimensional cross section of unpolarized DIS on the Born level has the following dependence on ϕ_h:

$$\sigma_0 = \frac{d\sigma_0}{dxdydzdp_t^2 d\phi_h} = \frac{N}{Q^4}(A + \cos\phi_h A^c + \cos 2\phi_h A^{cc}), \tag{41}$$

where $N = \alpha^2 y S_x/\sqrt{\lambda_Q}$. The coefficients A, A^c and A^{cc} do not depend on ϕ_h more and they have the form

$$\begin{aligned} A &= 2Q^2\mathcal{H}_1 + (SX - M^2Q^2)\mathcal{H}_2 + (4a^1a^2 + 2b^2 - M_h^2Q^2)\mathcal{H}_3 \\ &\quad +(2Xa^1 + 2Sa^2 - zS_xQ^2)\mathcal{H}_4, \\ A^c &= 2b(2a^+\mathcal{H}_3 + S_p\mathcal{H}_4), \\ A^{cc} &= 2b^2\mathcal{H}_3. \end{aligned} \tag{42}$$

The model for structure functions $\mathcal{H}_i$ can be constructed on basis of results of the paper Mulders and Tangerman [62]. Keeping only the leading twist contribution we have for structure functions

$$\mathcal{H}_1 = \sum_q e_q^2 f_q(x) D_q\mathcal{G}, \quad \mathcal{H}_2 = -\frac{p_t^2 + m_h^2}{M^2E_h^2}\sum_q e_q^2 f_q(x) D_q\mathcal{G}, \\ \mathcal{H}_3 = 0 \qquad\qquad \mathcal{H}_4 = \frac{1}{ME_h}\sum_q e_q^2 f_q(x) D_q\mathcal{G}, \tag{43}$$

and

$$\mathcal{G} = \mathcal{G}_1 = b\exp(-bp_t^2), \tag{44}$$

where $b = R^2/z^2$ is a slope parameter and R is a parameter of the model. Alternatively power fit is also considered in [11].

When integrated over the kinematic variables ϕ_h and p_t the cross section (41) coincides with the unpolarized part of semi-inclusive cross section calculated within quark parton model (35).

The cross section that takes into account radiative effects can be written as

$$\sigma_{obs} = \sigma_0 e^{\delta_{inf}}(1+\delta_{VR}+\delta_{vac}) + \sigma_F. \tag{45}$$

Here the corrections δ_{inf} and δ_{vac} come from radiation of soft photons [12] and effects of vacuum polarization[2]. The correction δ_{VR} is infrared free sum of factorized parts of real and virtual photon radiation. These quantities are given by the following expressions

$$\begin{aligned}
\delta_{VR} &= \frac{\alpha}{\pi}\Big(\frac{3}{2}l_m - 2 - \frac{1}{2}\ln^2\frac{X'}{S'} + \mathrm{Li}_2\frac{S'X'-Q^2p_x^2}{S'X'} - \frac{\pi^2}{6}\Big), \\
\delta_{inf} &= \frac{\alpha}{\pi}(l_m-1)\ln\frac{(p_x^2-(M+m_\pi)^2)^2}{S'X'}, \\
\delta_{vac} &= \delta_{vac}^{lept} + \delta_{vac}^{hadr},
\end{aligned} \tag{46}$$

where $S' = X + Q^2 - V_2$, $X' = S - Q^2 - V_1$, $l_m = \ln Q^2/m^2$ and Li_2 is Spence function or dilogarithm.

The contribution of radiative tail has the standard form (see eq.(12))

$$\sigma_F = -\frac{\alpha N}{2\pi}\int\limits_0^{2\pi} d\phi_k \int\limits_{\tau_{min}}^{\tau_{max}} d\tau \sum_{i=1}^{4}\sum_{j=1}^{3}\theta_{ij}(\tau,\phi_k) \int\limits_0^{R_{max}} dR R^{j-2}\Big[\frac{\mathcal{H}_i}{(Q^2+R\tau)^2} - \delta_j\frac{\mathcal{H}_i^0}{Q^4}\Big]. \tag{47}$$

Here $2M^2\tau_{max,min} = S_x \pm \sqrt{\lambda_Q}$ and $R_{max} = (M_x^2-(M+m_\pi)^2)/(1+\tau-\mu)$, δ_j=1 for j=1 and δ_j=0 otherwise. The explicit formulae for functions $\theta(\tau,\phi_k)$ can be found in [11]. The structure functions $\mathcal{H}_i^0$ have to be calculated for Born kinematics, but $\mathcal{H}_i$ is calculated in terms of tilde variables introducing by

$$\begin{aligned}
\tilde{Q}^2 &= (q-k)^2 = Q^2 + R\tau, \\
\tilde{W}^2 &= (p+q-k)^2 = W^2 - R(1+\tau), \\
\tilde{t} &= (q-k-p_h)^2 = t + R(\tau-\mu), \\
\tilde{M}_x^2 &= \tilde{p}_x^2 = M_x^2 + R(1+\tau-\mu).
\end{aligned} \tag{48}$$

1.4 Higher order effects

The dominant contribution to RC can be obtained by the method of leading logarithms. Being based on the fermion mass factorization this approximation allows us to calculate corrections $\sim(\alpha\log(Q^2/m_f^2))^n$. The below formulae were obtained in [44] by the method which is presented in [43].

The contribution of inelastic tail σ_2^{in} together with loop effects σ_2^v

$$\sigma_2^{in}+\sigma_2^v = \delta_2^{in}\sigma_0 + \sigma_{Vk_1}^{in} + \sigma_{Vk_2}^{in} + \sigma_{k_1k_1}^{in} + \sigma_{k_2k_2}^{in} + \sigma_{k_1k_2}^{in} + \sigma_{lk_1}^{in} + \sigma_{lk_2}^{in} + \sigma_{fk_1}^{in} + \sigma_{fk_2}^{in}. \tag{49}$$

The factorized part is

$$\delta_2^{in} = \frac{\alpha^2}{4\pi^2}(3\delta^2(Q^2) + 2l_m\delta_{sp}\delta(Q^2)) + \frac{1}{2}l_m^2[\delta_{sp}^2 + 4\mathrm{Li}_2(1-z_2) + 12\mathrm{Li}_2(1-z_1) - \frac{8}{3}\pi^2]), \tag{50}$$

[2]There are explicit formulae for leptonic contribution to vacuum polarization effect (see [13] for example) and parameterization of hadronic one [55].

$l_m = \log Q^2/m^2$, $\delta_{sp} = 2\log((1-z_1)(1-z_2)) + 3$, and $\delta(Q^2) = \delta^l_{vac} + \delta^h_{vac}$.

The contribution from the vacuum polarization if it coincides with real photon radiation has the form

$$\sigma^{in}_{Vk_1,Vk_2} = \frac{\alpha^2}{2\pi^2} l_m \int\limits_{z_{1,2}}^{1} \frac{dz}{1-z} \left[(1+z^2)\delta(t_{x,s})\sigma_{s,p} - 2\delta(Q^2)\sigma_0 \right], \tag{51}$$

where $t_x = zQ^2$ and $t_s = Q^2/z$.

Next three terms correspond to the cases when two radiated photons are collinear to an incident electron ($\sigma_{k_1k_1}$), an outgoing electron ($\sigma_{k_2k_2}$)

$$\begin{aligned} \sigma^{in}_{k_1k_1,k_2k_2} = \frac{\alpha^2}{8\pi^2} l_m^2 \int\limits_{z_{1,2}}^{1} dz \Bigg[\frac{2}{1-z} (2\log[(1-z)(1-z_{1,2}(z))] - \ln z + 3) \times \\ \times ((1+z^2)\sigma_{k_{1,2}} - 2\sigma_0) + ((1+z)\ln z - 2(1-z))\sigma_{k_{1,2}} \Bigg], \end{aligned} \tag{52}$$

or when one photon is radiated in incident electron direction and the other in the outgoing electron direction ($\sigma_{k_1k_2}$):

$$\begin{aligned} \sigma^{in}_{k_1k_2} = \frac{\alpha^2}{4\pi^2} l_m^2 \int\limits_{z_1}^{1} \frac{dz'}{1-z'} \int\limits_{z_2(z')}^{1} \frac{dz}{1-z} \Bigg[(1+z^2)(1+z'^2)\sigma_{k_1k_2} - 2(1+z'^2)\sigma_{k_1} \\ -2(1+z^2)\sigma_{k_2} + 4\sigma_0 \Bigg]. \end{aligned} \tag{53}$$

Here

$$\begin{aligned} \sigma_{k_1k_2} = y\sigma_0(z'S, X/z, z'Q^2/z)/(z(zz'-1+y)), \\ z_1(z) = (1-y)/(z-xy), z_2(z) = (1-y+zxy)/z. \end{aligned} \tag{54}$$

There are two channels (singlet and non-singlet) of the fermion pair production that give a contribution to α^2 of order RC. The singlet channel

$$\sigma^{in}_{lk_1,lk_2} = \frac{\alpha^2}{8\pi^2} l_m^2 \int\limits_{z_{1,2}}^{1-4m_lM/S} dz(2(1+z)\log z + 1 - z + \frac{4}{3}(1-z^3)z)\sigma_{k_{1,2}} \tag{55}$$

corresponds to the case when the incident and the outgoing lepton as well as the leptons of the unregistered pair belong to different leptonic lines connected by an additional virtual photon.

The rest non-singlet part

$$\sigma^{in}_{fk_1,fk_2} = \frac{\alpha^2}{12\pi^2} \sum_f \log^2 \frac{Q^2}{m_f^2} \int\limits_{z_{1,2}}^{1-4m_fM/S} dz \frac{(1+z^2)}{(1-z)} \sigma_{k_{1,2}} \tag{56}$$

arises from the two-lepton decay of an additional virtual photon.

The main contribution to the second order elastic and quasielastic radiative tail arises when the additional radiated photon is collinear to the incident or outgoing fermion line:

$$\sigma_2^{el} = \frac{\alpha}{2\pi} l_m \delta_{sp} \sigma_1^{el} + \sigma_{k_1 t}^{el} + \sigma_{k_2 t}^{el}, \tag{57}$$

where

$$\sigma_{k_{1,2}t}^{el} = \frac{\alpha}{2\pi} l_m \int\limits_{z_{1,2}}^{1} dz \frac{(1+z^2)\sigma_{k_{1,2}}^{el} - 2\sigma_1^{el}}{1-z}. \tag{58}$$

The quantities $\sigma_{k_{1,2}}^{el}$ are obtained in the terms of approximate elastic radiative tail $\sigma_1^{el} = \sigma_1^{el}(x,y,S)$:

$$\begin{aligned} \sigma_{k_1}^{el} &= y\sigma_1^{el}(xyz/(z+y-1), (z+y-1)/z, zS)/(z-1+y), \\ \sigma_{k_2}^{el} &= y\sigma_1^{el}(xy/(z+y-1), (z+y-1)/z, S)/z(z-1+y). \end{aligned} \tag{59}$$

The numerical analysis shown that correction $\sim \alpha^2$ to the considered asymmetry is about some per cent from the full RC and has a maximum near kinematic borders of the considered experiments.

However it is necessary to remind that correction $\sim \alpha^2$ has been calculated within LO approximation while even ultrarelativistic approximation for radiative tails from elastic and quasielastic peaks leads to high corrections. Besides, the approximation $\sim \alpha^2 \log^2(Q^2/m^2)$ gives rather good results for the factorizad part of correction but it produce poorer ones for the remaining components which make the dominant contribution to the asymmetry in polarized particle scattering. Hence, a more accurate calculation is required for more detail analysis of $\sim \alpha^2$ correction.

1.5 FORTRAN codes POLRAD 2.0 and HAPRAD

Using the results presented in the previous subsections two FORTRAN code POLRAD 2.0 [14] and HAPRAD [11] have been created. Here some results obtained by these codes are presented.

The program POLRAD 2.0 consists of two patches. The first one which itself is called POLRAD describes RC to inclusive DIS. In order to estimate some radiative effects by this patch let us separate cross section into spin-averaged and spin-dependent parts

$$\sigma_{0,1,2} = \sigma_{0,1,2}^{u} + P_N \sigma_{0,1,2}^{p}. \tag{60}$$

and consider the following quantities:

$$\delta_1^{u,p} = \frac{\sigma_0^{u,p} + \sigma_1^{u,p}}{\sigma_0^{u,p}}, \qquad \delta_2^{u,p} = \frac{\sigma_0^{u,p} + \sigma_1^{u,p} + \sigma_2^{u,p}}{\sigma_0^{u,p}}, \tag{61}$$

which are characterized the ratio of the total unpolarized and polarized part of the cross section to the Born one (with and without second order effect). The dependence of these quantities on scaling variable in HERMES kinematics is presented in fig. 4.

The second patch of POLRAD 2.0 which is called as SIRAD allows us to calculate RC to three-dimension cross section $d\sigma/dxdydz$ of semi-inclusive DIS. Fig. 5 shows the ratio

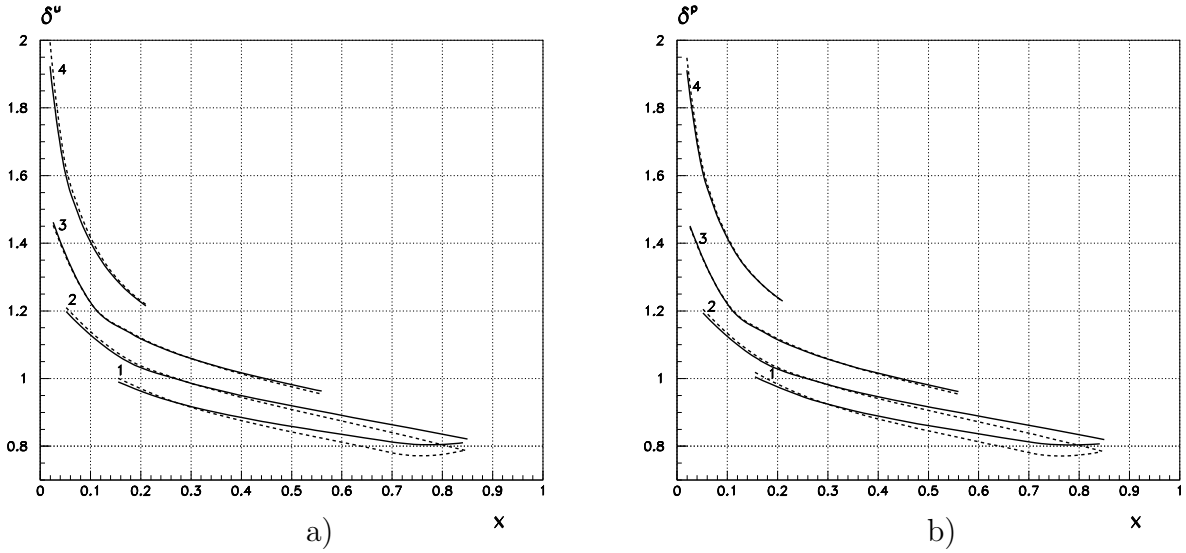

Figure 4: *$x-$dependence of the ratio of the total cross section to the Born on with (dashed curves) and without (solid curves) the second order effects for electron-proton DIS with HERMES kinematics at the initial lepton energy of $E_e = 27.5GeV$ for 1) $y = 0.1$, 2) $y = 0.3$, 3) $y = 0.6$, 4) $y = 0.8$; a)the correction to unpolarized part of cross section; b)the correction to polarized part of cross section.*

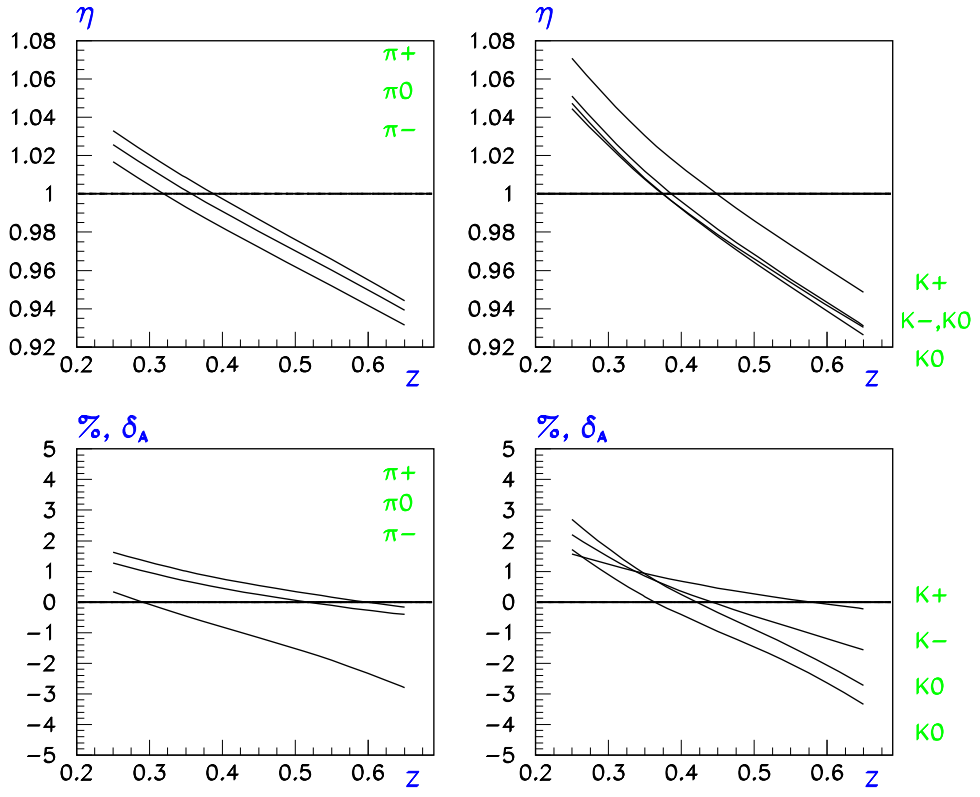

Figure 5: *The radiative correction factor to semi-inclusive cross sections ($\eta = \sigma/\sigma_0$, upper plots) and to polarization asymmetry ($\delta_A = (A^{obs} - A^{born})/A^{born}$, lower plots) versus z. The cross sections were integrated over other kinematic variables within HERMES cuts [63].*

x	y	Q^2 GeV^2	z	SIRAD	HAPRAD					
					without cuts			with cuts		
					$\mathcal{G}_1$	$\mathcal{G}_1'$	$\mathcal{G}_2$	$\mathcal{G}_1$	$\mathcal{G}_1'$	$\mathcal{G}_2$
0.038	0.677	1.33	0.25	1.029	1.033	1.024	0.982	1.041	1.025	0.985
0.062	0.567	1.82	0.35	0.996	0.989	0.989	0.947	0.989	0.980	0.951
0.092	0.529	2.52	0.45	0.970	0.961	0.961	0.934	0.961	0.956	0.936
0.131	0.499	3.38	0.55	0.945	0.936	0.933	0.912	0.934	0.931	0.906
0.198	0.476	4.88	0.65	0.918	0.902	0.902	0.889	0.897	0.897	0.881

Table 1: *The results for RC factors to three dimensional semi-inclusive cross section obtained by FORTRAN codes SIRAD and HAPRAD (see text for further explanations). Kinematic points are taken from the Table 1 in ref. [63].*

$\eta = \sigma^{obs}/\sigma^{born}$ and the relative correction to asymmetry $\delta_A = (A^{obs} - A^{born})/A^{born}$ for K and π mesonproduction.

To estimate the RC to five-dimensional cross section $d^5\sigma/dxdydzdp_t^2d\theta_h$ the special FORTRAN code HAPRAD was developed. Now we show that numerical results for RC to $d\sigma/dxdydz$ reproduced by these two codes which coincide with a good accuracy. It can be seen in the Table 1 where we represent RC to the cross section as it follows from the runs of the codes POLRAD 2.0 and HAPRAD. Since HAPRAD allows us to take into account the kinematic cuts and to use different models for p_t^2-slope, three fits for p_t^2-distribution and the cases with and without experimental cuts were considered. The first fit for p_t^2-slope is defined in (44), while the second and third ones are our fits of experimental data [64] using exponential ($\mathcal{G}_1' = \mathcal{G}_1$ at $b = a/z$) and power functional forms

$$\mathcal{G} = \mathcal{G}_2 = \left[\frac{1}{a + bz + p_t^2}\right]^{c+dz}. \tag{62}$$

As the kinematic cuts on ϕ_h and p_t of the measured hadron we took HERMES geometrical cuts [65]. We can conclude from this analysis that neither important differences between SIRAD and HAPRAD results, if exponential model for p_t^2-distribution is used, nor dependence on slope parameter model and applying of geometrical cuts are found. However RC takes a negative shift in the model based on power functional form (62). As it is shown in [11] RC depends on steepness of p_t^2 distribution. It is a reason why models like $\delta(p_t^2)$ (QPM, POLRAD 2.0) and (44) give larger RC. Within practical RC procedure in concrete measurement of $d\sigma/dxdydz$ the model can be fixed only if the information about p_t^2-distribution is additionally considered.

1.6 Monte Carlo generator RADGEN 1.0

In this subsection we present a Monte Carlo generator RADGEN 1.0 [15] for the events with a possible radiation of a real photon in DIS on polarized and unpolarized targets. The events are generated in accordance with their contribution to the observed total cross section given by

$$\sigma_{obs} = \sigma_{non-rad}(\Delta) + \sigma_{in}(\Delta) + \sigma_q + \sigma_{el}. \tag{63}$$

The first term $\sigma_{non-rad}(\Delta)$ contains not only the contribution from the Born process but the contributions from loop corrections (σ_v) and from multiple soft photon production with a total energy not exceeding a cut-off parameter Δ. In handling the radiative corrections two approaches have been used, the one developed by Mo and Tsai [1, 2] and the other given by Bardin and Shumeiko [3].

Kinematics of the Born (or one photon exchange) process is completely defined by the scattering angle θ and the energy E' of the scattered lepton, two variables which are usually measured. All other inclusive kinematic variables can be expressed in the terms of θ and E'. Having in mind the laboratory frame, i.e. the frame with the target nucleus at rest the relevant variables are

$$\begin{aligned} Q^2 = 4EE'\sin^2\frac{\theta}{2}, \qquad \nu = E - E', \qquad x = \frac{Q^2}{2M\nu}, \\ y = \frac{\nu}{E}, \qquad W^2 = Q^2(1/x - 1) + M^2, \end{aligned} \tag{64}$$

where E is the beam energy.

The event registered in the detector with certain values of E' and θ for the scattered lepton can either be a non-radiative or a radiative event, i.e. an event containing a real hard radiated photon. For the radiative event there are three additional variables necessary to fix the kinematics of the radiated real photon apart from E' and θ. A possible choice is the photon energy E_γ and the two angles θ_γ and ϕ_γ, where θ_γ is the angle between the real and the virtual photon momenta $\vec{k}$ and $\vec{q} = \vec{k}_1 - \vec{k}_2$ and ϕ_γ is the angle between the planes defined by the momenta ($\vec{k}_1$, $\vec{k}_2$) and ($\vec{k}$, $\vec{q}$). For the events with the radiation of a real photon the kinematic variables describing the virtual photon and which is used to generate the hadronic final state is derived from eq.(64) because the substitution $q \to q - k$ has to be made in their definition. The variables obtained after this substitution will be referred to as 'true' ones:

$$\begin{aligned} W^2_{true} = W^2 - 2E_\gamma(\nu + M - \sqrt{\nu^2 + Q^2}\cos\theta_\gamma), \quad \nu_{true} = \nu - E_\gamma, \\ Q^2_{true} = Q^2 + 2E_\gamma(\nu - \sqrt{\nu^2 + Q^2}\cos\theta_\gamma), \qquad x_{true} = \frac{Q^2_{true}}{2M\nu_{true}}. \end{aligned} \tag{65}$$

For non-radiative events the true kinematics exactly coincide with (64).

In case of the elastic and quasielastic radiative processes the mass squared of the hadronic final state is fixed imposing additional constraints on the true kinematic variables. Indeed the following ranges are allowed:

$$\begin{cases} x \le x_{true} \le 1 \quad \text{for } \sigma_{in} \\ x_{true} = 1 \quad \text{for } \sigma_q \qquad Q^2_{min} \le Q^2_{true} \le Q^2_{max} \\ x_{true} = M_A/M \quad \text{for } \sigma_{el} \end{cases} \tag{66}$$

where

$$Q^2_{max,min} = Q^2\frac{2(1 - x_r)(1 \pm \sqrt{1 + \gamma^2}) + \gamma^2}{\gamma^2 + 4x_r(1 - x_r)} \tag{67}$$

and

$$\gamma^2 = 4M^2x^2/Q^2, \qquad x_r = x/x_{true}. \tag{68}$$

The Monte-Carlo procedure for the generation of events with a possible photon radiation is the following:
The procedure starts off with the generation of the kinematics of the scattered lepton and the calculation of an event weight from these kinematics. Then the appropriate scattering channel (non-radiative; elastic, quasielastic or inelastic radiative tail) has to be chosen according to their contribution to the total observed cross section (see (63)). If a radiative channel is selected the radiated photon has to be generated and the values of the kinematic variables have to be re-computed to obtain the true values. For each event the weight has to be recalculated. The new weight is defined as the ratio of the radiatively corrected and the Born cross section. After this recalculation the weighted sum of all events (generated originally in accordance with the Born cross section) gives the observed cross section.

The recalculation of the weight requires the knowledge of the cross section integrated over the photon momentum. This is done differently in two theoretical approaches. In the Mo-Tsai approach an additional parameter Δ dividing the integration region into a soft and a hard photonic part is introduced. There is no such parameter in the Bardin-Shumeiko approach. However, in both approaches a minimal photon energy E^{γ}_{min} is adapted in generating a radiated photon. If the photon energy is above this value the kinematics of the photon is calculated and the event becomes a radiative one. The actual value of E^{γ}_{min} depends on the aim of the photon generator. In general photons should be detected in the calorimeter. So the energy threshold of the calorimeter sets the value for E^{γ}_{min}.

The unpolarized generator is based on the FORTRAN code FERRAD35 [66]. The code calculates the radiative correction to deep inelastic scattering of unpolarized particles in accordance with the analytical formulae given by Mo and Tsai [1, 2].

The result for the lowest order radiative correction of the cross section is

$$\sigma = \delta_R(\Delta)(1 + \delta_{vert} + \delta_{vac} + \delta_{sm})\sigma_{1\gamma} + \sigma_{el} + \sigma_q + \sigma_{in}(\Delta), \tag{69}$$

where $\sigma_{1\gamma}$ is the one photon exchange Born cross section and δ_{vac}, δ_{vert}, and δ_{sm} are corrections due to vacuum polarization by electron and muon pairs, vertex corrections and residuum of the cancellation of infrared divergent terms independent of Δ (see [15] for detail).

The cross sections σ_{el}, σ_q, and σ_{in} are the contributions from radiative processes (i.e. including real photon radiation) for elastic, quasielastic and deep inelastic scattering (see [1, 2, 15] for detail).

An artificial parameter Δ had to be introduced to divide the integration region over the photon energy into two parts, the soft and the hard energy regions. The hard energy region $\sigma_{in}(\Delta)$ can be calculated without any approximations. The soft photon part is calculated for photon energies approaching zero. After cancellation of the infrared divergences and a resummation of soft multiphoton effects the correction factor is given by

$$\delta_R(\Delta) = \exp\left[-\frac{\alpha}{\pi}\left(\ln\frac{E}{\Delta} + \ln\frac{E'}{\Delta}\right)\left(\ln\frac{Q^2}{m^2} - 1\right)\right]. \tag{70}$$

The polarized generator is constructed utilizing the FORTRAN code POLRAD 2.0 [13,14] that was presented above. The cross section formulae (9-18) can be rewritten into a form similar to eq.(69):

$$\sigma = \delta_R(E^\gamma_{min})(1+\delta_{vert}+\delta_{vac}+\delta_{sm})\sigma_{1\gamma} + \sigma_{add}(E^\gamma_{min}) + \sigma_{el} + \sigma_q + \sigma_{in}(E^\gamma_{min}). \quad (71)$$

In the ultrarelativistic approximation ($Q^2 \gg m^2$) the corrections δ_{vert}, δ_{vac}, and δ_{sm} take the same form as in eq.(69) [3]. Since this code is based on the method of covariant cancellation of infrared divergences developed by Bardin and Shumeiko [3] the final formula for the cross section free of infrared divergences does not include any artificial parameter like Δ. However, E^γ_{min} has to be introduced if the code is used considering the generation of real radiated photons. As a result the formula (12) has to be rewritten in the following way

$$\sigma_{in} = -\alpha^3 y \int\limits_{\tau_{min}}^{\tau_{max}} d\tau \sum_{i=1}^{4}\sum_{j=1}^{k_i} \theta_{ij}(\tau) \int\limits_{R_{min}}^{R_{max}} dR \frac{R^{j-2}}{(Q^2+R\tau)^2} \Im_i(R,\tau), \quad (72)$$

while the elastic and quasielastic radiative tails were defined above by eq.(16) and (18) respectively. The lower integration limits is determined by $R_{min} = 2ME^\gamma_{min}$.

Apart from the usual ultrarelativistic approximation another one was made when the eqs. (69) and (31) were obtained, namely the photon energy was considered to be small $E^\gamma \ll E, E'$ in the region $E^\gamma < E^\gamma_{min}$. In POLRAD, the term $\sigma_{add}(E^\gamma_{min})$ is added to take the difference of this approximation to the exact formula into account:

$$\begin{aligned}\sigma_{add}(E^\gamma_{min}) &= -\alpha^3 y \int\limits_{\tau_{min}}^{\tau_{max}} d\tau \sum_{i=1}^{4} \Bigg\{ \theta_{i1}(\tau) \int\limits_{0}^{2ME^\gamma_{min}} \frac{dR}{R} \left[\frac{\Im_i(R,\tau)}{(Q^2+R\tau)^2} - \frac{\Im_i(0,0)}{Q^4} \right] \\ &\quad + \sum_{j=2}^{k_i} \theta_{ij}(\tau) \int\limits_{0}^{2ME^\gamma_{min}} dR \frac{R^{j-2}}{(Q^2+R\tau)^2} \Im_i(R,\tau) \Bigg\} \quad (73)\end{aligned}$$

Therefore, the results obtained with the help of POLRAD are independent of the threshold parameter E^γ_{min} by construction.

To estimate the value of radiative effects numerically Monte-Carlo event samples of 100k events each have been generated for a ^{3}He target and kinematic cuts relevant for the HERMES experiment [67] have been applied (Q^2 >1 GeV^2, W^2 >4 GeV^2, y <0.85, 0.037< θ <0.14rad). The distributions of the radiation angles θ_γ and ϕ_γ as defined in the so-called Tsai-system in which the z-axis is along the direction of the virtual photon and the y-axis is normal to the scattering plane (see ref. [1,2]) and of the energy E_γ are displayed in fig.6. These distributions are generated for a certain point in the kinematic plane of the scattered lepton, i.e. for $x = 0.1$ and $y = 0.8$. The two peaks seen in the θ_γ distribution of fig.6 correspond to the s- and p-peak emerging from collinear radiation along the direction of the incoming and outgoing lepton, respectively.

[3]It should be noted that contributions from τ-leptons and quark loops were included into δ_{vac} [13].

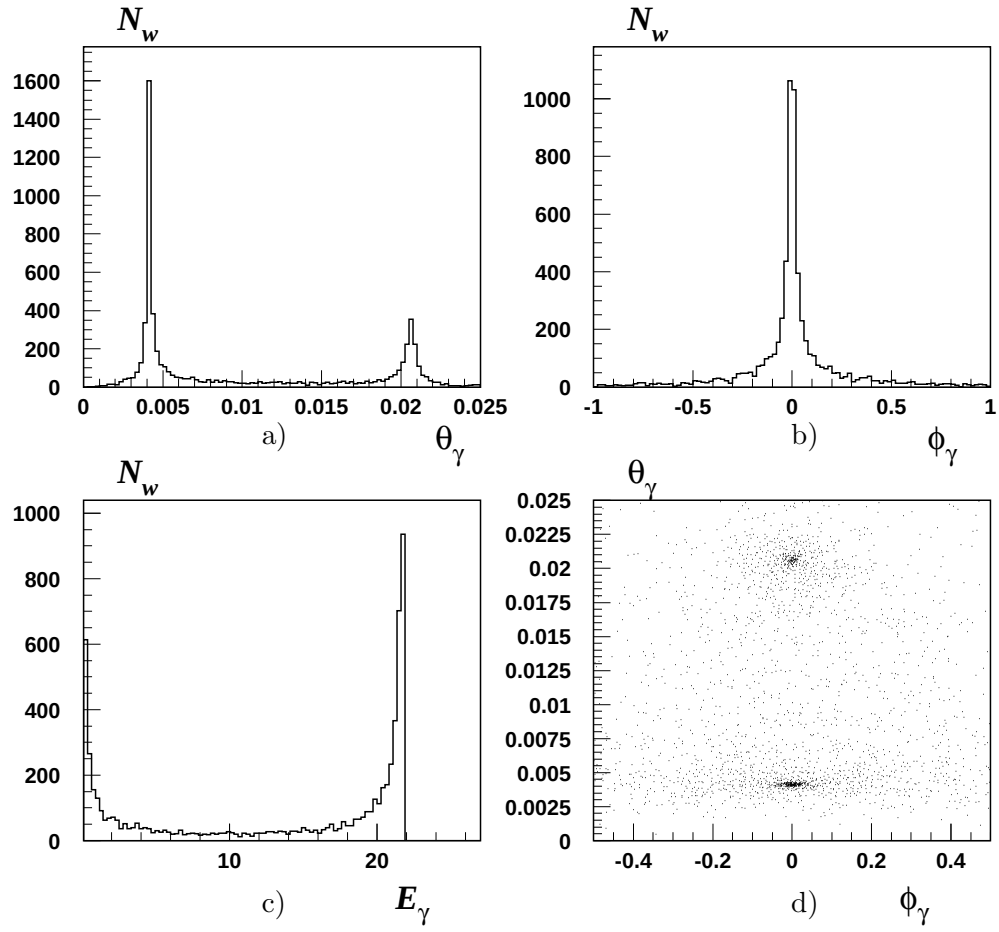

Figure 6: *The distribution of the radiation angles θ_γ a) and ϕ_γ b) and of the energy c) of the radiated photon for $x = 0.1$ and $y = 0.8$. The two-dimensional distribution d) shows θ_γ vs ϕ_γ.*

1.7 Electroweak correction

It is natural, that data processing of modern experiments on DIS requires correct account of RC. The above presented expressions for RC to polarized DIS within QED is successfully used for fixed target experiments.

However when the polarization DIS experiments at collider will be possible [27], we cannot restrict our consideration to γ-exchange graphs only, because in this case the squared transfer momentum Q^2 is so high that weak effects begin to play an essential role in the total cross section and spin asymmetries. At the same time the ratio m^2/Q^2 (where m is the mass of a scattering lepton) becomes so small that it could be restricted to non-vanishing terms for $m \to 0$. The such calculation was already done by us [37], but there we used only the naive parton model.

In this subsection the electroweak correction to the lepton currents within QCD-improved parton distribution.

Generally, the double differential cross section lepton-nucleon scattering in the frame

electroweak theory has a form

$$\sigma_0 = \frac{4\pi\alpha^2 S_x S}{\lambda_s Q^4}\left[L^{\gamma\gamma}_{\mu\nu}W^{\gamma\gamma}_{\mu\nu}(p,q) + \frac{1}{2}(L^{\gamma Z}_{\mu\nu} + L^{Z\gamma}_{\mu\nu})W^{\gamma Z}_{\mu\nu}(p,q)\chi L^{ZZ}_{\mu\nu}W^{ZZ}_{\mu\nu}(p,q)\chi^2\right], \qquad (74)$$

where $\chi = Q^2/(Q^2 + M_Z^2)$ (M_Z is the Z-boson mass), while the explicit expression for leptonic $L^{ij}_{\mu\nu}$ and hadronic $W^{ij}_{\mu\nu}$ tensor ($i, j = \gamma, Z$) can be found in [32].

After tensor contractions cross section (74) can be written in more simple form

$$\sigma_0 = \frac{4\pi\alpha^2 y}{Q^4}\sum_{i=1}^{8}\theta_i^B\mathcal{F}_i \qquad (75)$$

through linear combination eight generalized structure functions:

$$\begin{aligned}\mathcal{F}_i &= R_V^\gamma\bar{F}_i^\gamma + \chi R_V^{\gamma Z}\bar{F}_i^{\gamma Z} + \chi^2 R_V^Z\bar{F}_i^Z \qquad (i = 1, 2, 6-8),\\ \mathcal{F}_i &= R_A^\gamma\bar{F}_i^\gamma + \chi R_A^{\gamma Z}\bar{F}_i^{\gamma Z} + \chi^2 R_A^Z\bar{F}_i^Z \qquad (i = 3-5).\end{aligned} \qquad (76)$$

Here the quadratic combinations of the electroweak coupling constants are defined as:

$$\begin{aligned}R_V^{mn} &= (v^m v^n + a^m a^n) - P_L(v^m a^n + v^n a^m),\\ R_A^{mn} &= (v^m a^n + a^m v^n) - P_L(v^m v^n + a^n a^m),\end{aligned} \qquad (77)$$

where

$$\begin{aligned}v^\gamma &= 1, \qquad & v^Z &= (-1 + 4s_w^2)/4s_w c_w,\\ a^\gamma &= 0, \qquad & a^Z &= -1/4s_w c_w,\end{aligned} \qquad (78)$$

c_w and s_w are cosin and sine of Weinberg's angle respectively and P_L is degree of lepton polarization. The quantities θ_i^B depend only on the target polarization vector and kinematic invariants:

$$\begin{aligned}\theta_1^B &= Q^2, & \theta_5^B &= \eta q Q^2 S_p/2M^3,\\ \theta_2^B &= (SX - M^2Q^2)/2M^2, & \theta_6^B &= -(X\eta k_1 + S\eta k_2)/2M,\\ \theta_3^B &= Q^2 S_p/4M^2, & \theta_7^B &= \eta q(SX - M^2Q^2)/2M^3,\\ \theta_4^B &= -Q^2\eta(k_1 + k_2)/M, & \theta_8^B &= -\eta q Q^2/M.\end{aligned} \qquad (79)$$

Model independent part of lowest-order electroweak correction which includes contributions both from a real photon emission (σ_R), and from the additional virtual particles (σ_V) can be presented as a sum of infrared free terms:

$$\sigma_{RC} = \sigma_V + \sigma_R = \frac{\alpha}{\pi}\delta_{VR}\sigma_0 + \sigma_V^r + \sigma_R^F + \hat{\sigma}_R. \qquad (80)$$

The factor

$$\begin{aligned}\delta_{VR} = \quad & (\log\frac{Q^2}{m^2} - 1)\ln\frac{(W^2 - (M + m_\pi)^2)^2}{(X + Q^2)(S - Q^2)} + \frac{3}{2}\log\frac{Q^2}{m^2} - 2\\ & -\frac{1}{2}\log^2\frac{X + Q^2}{S - Q^2} + \mathrm{Li}_2\frac{SX - Q^2M^2}{(X + Q^2)(S - Q^2)} - \frac{\pi^2}{6}\end{aligned} \qquad (81)$$

appears in front of the Born cross section after cancellation of infrared divergence by summing of an infrared part separated from σ_R and that part of virtual contribution which arises from the lepton vertex graphs including an additional virtual photon.

The contribution from electroweak rest loop correction can be written in terms of the Born cross section with the following replacement:

$$\sigma_V^r = \sigma^B \left(R_{V,A}^{mn} \to \delta R_{V,A}^{mn} \right), \tag{82}$$

and $\delta R_{V,A}^{mn}$ defined in [32].

The infrared free part of the cross section of the radiative process can be presented as a sum of two terms σ_R^F and $\hat{\sigma}_R$. The first term includes unpolarized part of the cross section as well as that part of cross section which appears from leading term ξ_0 of lepton polarization vector (5). It looks like eq. (12)

$$\begin{aligned}\sigma_R^F = \quad & \alpha^3 y \int\limits_{\tau_{min}}^{\tau_{max}} d\tau \sum_{i=1}^{8} \Big\{ \theta_{i1}(\tau) \int\limits_0^{R_{max}} \frac{dR}{R} \left[\frac{\mathcal{F}_i(R,\tau)}{(Q^2+R\tau)^2} - \frac{\mathcal{F}_i(0,0)}{Q^4} \right] \\ & + \sum_{j=2}^{k_i} \theta_{ij}(\tau) \int\limits_0^{R_{max}} dR \frac{R^{j-2}}{(Q^2+R\tau)^2} \mathcal{F}_i(R,\tau) \Big\}. \end{aligned} \tag{83}$$

where the integration variables and their limits are defined by formulae (13,14). The second term containing the contribution which is proportional to the rest part of polarization vector ξ_1 in the limit $m \to 0$ can be written through the Born cross section:

$$\hat{\sigma}_R = \frac{\alpha y}{\pi S} \int\limits_0^{R_{max}^s} \frac{R dR}{(S_x - R)} \tilde{\sigma}_{pl}^B. \tag{84}$$

The upper integration limit defines as $R_{max}^s = S(W^2 - (M+m_\pi)^2)/(S-Q^2)$, and $\tilde{\sigma}_{pl}^B$ is the proportional P_L part of the Born cross section with the following replacement kinematic variable: $S \to S - R$, $Q^2 \to Q^2(1 - R/S)$ and $k_1\eta \to k_1\eta(1 - R/S)$.

The double differential cross section as a function of the polarization characteristics of the scattering particles can be presented as the sum of four terms:

$$\sigma = \sigma^u + P_L\sigma^\xi + P_N\sigma^\eta + P_N P_L \sigma^{\xi\eta}, \tag{85}$$

the first of them is an unpolarized cross section and three others characterize the polarized contributions independent on polarization degrees.There are no problems with the luminosity measurement in the current collider experiments, so apart from the usual measurement of polarized asymmetries the absolute measurement of the cross sections with different polarization configurations of beam and target will be probably possible in future polarization experiments at collider. Besides, now the new methods of data processing, when experimental information of spin observables is extracted directly from the polarized part of the cross section [68, 69] are actively developed. In [69] it is shown how to separate completely unpolarized and polarized cross sections from a sample of experimental data using a special likelihood procedure and a binnig on polarization degrees. All above mentioned as well as the fact that RC to asymmetry is always constructed from RC to

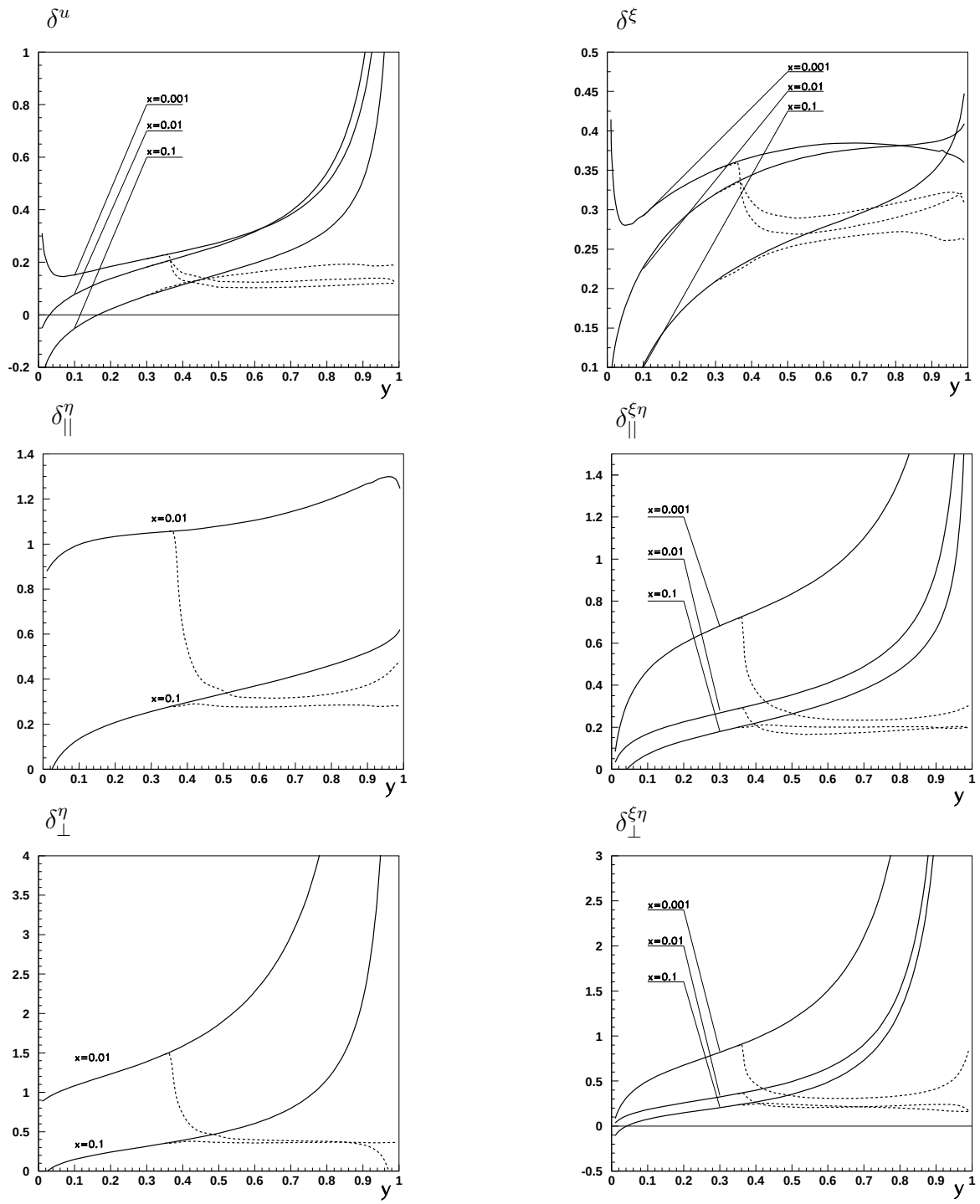

Figure 7: *Radiative correction to $\Delta\sigma$ defined in (86) with (dashed curves) and without cut (full curves). The down indexes $||$ and $\perp$ correspond to longitudinally and transversely polarized proton beam respectively.*

parts of the cross section allows to restrict our consideration to numerical studying of RC to all of the cross sections in the equation (85) and their combinations.

Radiative corrections to these cross sections defined as a ratio of the cross section including one-loop RC only to the Born one

$$\delta^a = \frac{\sigma^a_{RC}}{\sigma^a_B} = \frac{\sigma^a_{tot}}{\sigma^a_B} - 1, \qquad (a = u, \xi, \eta, \xi\eta) \tag{86}$$

is presented on fig. 7 as a function of scaling variables x and y. The kinematic region corresponds to the present unpolarization collider experiment at HERA [26].

In experiments at collider a detection of a hard photon in calorimeter is used to reduce radiative effects. The dashed lines on fig. 7 demonstrate the influence of an experimental cut on the RC. One of the simplest variant of the cut when events having a radiative photon energy $E_\gamma > 10$GeV are rejected from analysis, is considered only.

2 Correction to the hadronic current in DIS

2.1 Tools of calculation and explicit results

On the language of the hadronic tensor $W_{\mu\nu}$ the lowest-order one-loop RC to the hadronic current consists of two parts whose contributions are calculated in a different way: $W^{1-loop}_{\mu\nu} = W^R_{\mu\nu} + W^V_{\mu\nu}$. The first one appears from a gluon emission and requires the integration over its phase space, while the second part comes from a gluon exchange graph and reads

$$W^V_{\mu\nu} = \frac{4}{3}\frac{\alpha_s}{\pi}\sum_q \left[-2\left(\mathcal{P}^{IR} + \ln\frac{m_q}{\mu}\right)(l_q - 1) - \frac{1}{2}l_q^2 + \frac{3}{2}l_q - 2 + \frac{\pi^2}{6}\right] W^{0q}_{\mu\nu} + W^{AMM}_{\mu\nu}, \tag{87}$$

where $W^{0q}_{\mu\nu}$ is a contribution of q-quark to the hadronic tensor on the Born level, and $W^{AMM}_{\mu\nu}$ is the quark anomalous magnetic moment. The pole term which corresponds to the infrared divergence is contained in $\mathcal{P}^{IR}$. The arbitrary parameter μ has a dimension of a mass.

Both of these contributions include the infrared divergences, which have to be careful considered in order to be canceled. Like QED we use the identity

$$W^R_{\mu\nu} = W^R_{\mu\nu} - W^{IR}_{\mu\nu} + W^{IR}_{\mu\nu} = W^F_{\mu\nu} + W^{IR}_{\mu\nu}.$$

Here $W^F_{\mu\nu}$ is finite for $k \to 0$, and $W^{IR}_{\mu\nu}$ is the infrared divergent part of $W^R_{\mu\nu}$. Using the dimensional regularization scheme the latter can be given in the form

$$\begin{aligned} W^{IR}_{\mu\nu} &= \frac{4}{3}\frac{\alpha}{\pi}\sum_q \Big[2\Big(\mathcal{P}^{IR} + \ln\frac{m_q}{\mu}\Big)(l_q - 1) + l_q l_v + \frac{1}{2}l_q^2 \\ &\qquad - \frac{1}{2}l_v^2 - \frac{3}{4}l_q - \frac{7}{4}l_v + \frac{3}{4} - \frac{\pi^2}{3}\Big] W^{0q}_{\mu\nu}, \end{aligned}$$

where $l_q = \log(Q^2/m_q^2)$, $l_v = \log((1-x)/x)$. The sum of $W^{IR}_{\mu\nu}$ and $W^V_{\mu\nu}$

$$\begin{aligned} W^{IR}_{\mu\nu} + W^V_{\mu\nu} &= \frac{2}{3}\frac{\alpha_s}{\pi}\sum_q [2l_q l_v - l_v^2 + \frac{3}{2}l_q - \frac{7}{2}l_v - \frac{5}{2} - \frac{\pi^2}{3}] W^{0q}_{\mu\nu} + W^{AMM}_{\mu\nu} \\ &= \frac{2}{3}\frac{\alpha_s}{\pi}\sum_q \delta_q W^{0q}_{\mu\nu} + W^{AMM}_{\mu\nu} \end{aligned} \tag{88}$$

is infrared free.

In order to extract some information about QCD contribution to the polarized structure functions, the integration in $W^F_{\mu\nu}$ over the gluon phase space should be performed without any assumptions about the polarization vector η. So the technique of tensor integration have to be applied in this case. Since the result of the analytical integration has the same tensor structure as the usual hadronic tensor in polarized DIS, the coefficients in front of the corresponding tensor structures (like $g_{\mu\nu}$, $p_\mu p_\nu$ ...) can be interpreted as one-loop QCD contributions to the corresponding structure functions.

Thus the QCD-improved structure functions $F_{1,2,L}$ and g_1 read

$$F_1(x,Q^2) = \frac{1}{2x}[F_2(x,Q^2) - F_L(x,Q^2)], \qquad F_2(x,Q^2) = x\sum_q e_q^2 f_q(x,Q^2),$$

$$F_L(x,Q^2) = \frac{4\alpha_s}{3\pi} x\sum_q e_q^2 \int\limits_x^1 dz f_q(x/z), \qquad g_1(x,Q^2) = \frac{1}{2}\sum_q e_q^2 \Delta f_q(x,Q^2), \tag{89}$$

and g_2 looks like

$$g_2(x,Q^2) = \frac{\alpha_s}{6\pi}\sum_q e_q^2 \Big\{(1-2l_q-\ln(1-x))\Delta f_q(x) + \int\limits_x^1 dz\Big[(4l_q$$
$$-4\log z(1-z) - 12 - \frac{1}{(1-z)})\Delta f_q(x/z) + \frac{\Delta f_q(x)}{(1-z)}\Big]\Big\}, \tag{90}$$

where the Q^2-dependent unpolarized and polarized parton distributions are defined as

$$f_q(x,Q^2) = (1+\frac{2\alpha_s}{3\pi}\delta_q) f_q(x) + \frac{2\alpha_s}{3\pi}\int\limits_x^1 \frac{dz}{z}\Big[(\frac{1+z^2}{1-z}(l_q - \log z(1-z))$$
$$-\frac{7}{2}\frac{1}{1-z} + 3z + 4) f_q(\frac{x}{z}) - \frac{2}{1-z}\left(l_q + \log\frac{z}{1-z} - \frac{7}{4}\right) f_q(x)\Big],$$
$$\Delta f_q(x,Q^2) = (1+\frac{2\alpha_s}{3\pi}\delta_q) \Delta f_q(x) + \frac{2\alpha_s}{3\pi}\int\limits_x^1 \frac{dz}{z}\Big[(\frac{1+z^2}{1-z}(l_q - \log z(1-z))$$
$$-\frac{7}{2}\frac{1}{1-z} + 4z + 1) \Delta f_q(\frac{x}{z}) - \frac{2}{1-z}\left(l_q + \log\frac{z}{1-z} - \frac{7}{4}\right) \Delta f_q(x)\Big], \tag{91}$$

and δ_q can be found in (88).

It has to be noted that our formulae (89,90,91) are in the agreement with ones obtained earlier. The unpolarized structure functions coincide with (2.24,2.49) from [46], $g_1(x,Q^2)$ corresponds to the expression (13) in [47]. At last $g_2(x,Q^2)$ can be considered with the sum (18) and (19) from [48].

After integration of the QCD-improved structure functions over the scaling variable x it could be seen that QCD RC to the first moment of the unpolarized structure functions as well as g_2 have the identical values both for massive and massless quark approaches. However the value of QCD-correction to the first moment of g_1 depends on the scheme. It was calculated:

$$\int\limits_0^1 g_1(x,Q^2) = (1 - C_{g1}\frac{\alpha_s}{\pi}) \int\limits_0^1 dx g_1^0(x), \tag{92}$$

where $C_{g1} = 1$ for massless and $C_{g1} = 5/3$ for massive one.

2.2 Discussion and Conclusion

In this section we applied the approach traditionally used in QED and electroweak theory for calculation of QCD correction to the DIS structure functions and sum rules. Since the quark was considered massive within this approach, it allowed us to estimate the finite quark mass effects at the NLO level. LO correction contributes to the DIS structure functions but vanishes for the sum rules, so this mass effects are important just for the sum rules.

We found that there is no any additional effect for the first moment of the unpolarized structure functions as well as for g_2. However there is some non-zero correction to the first moment of g_1 and as a result to the Ellis-Jaffe and Bjorken sum rules. The value of the correction is in agreement with the results of refs. [47,50], obtained by different methods. We confirm also the statement of [47] that the classical value of correction to the first moment of g_1 is reproduced if we take into account the leading term of the polarization vector $\eta = p_{1q}/m_q$. However contrary to the paper we would interpret the result with $C_{g1} = 5/3$ in eqs.(92) as physical one. In our calculation we took the proton (quark) polarization vector in a general form. Using of the exact representation of the vector [13]:

$$\eta = \frac{1}{\sqrt{(k_1 p_{1q})^2 - m^2 m_q^2}} \Big[\frac{k_1 p_{1q}}{m_q} p_{1q} - m_q k_1 \Big] \tag{93}$$

leads to exactly the same result (with $C_{g1} = 5/3$) for the first moment of g_1. The second term giving the additional contribution $\sim 2/3$ cannot be neglected within the approximation under consideration. It can be easy understood from pure calculation of QED and electroweak corrections to the lepton current in DIS process [31], where the lepton polarization vector looks like hadron one (5). The explicit expression of this non-vanishing for $m \to 0$ contribution within electroweak correction to the lepton current is defined by the formula (84) from previous section. The more detailed description of this contribution treatment can be found in [32].

The result with $C_{g1} = 5/3$ was obtained under similar assumptions in the report [49]. The additional correction was discussed both within OPE (operator product expansion) and within improved quark-parton model in paper [50]. It was shown in this paper that there is no contradiction between this result and classical correction obtained for massless QCD, if we carefully take into account the finite quark mass effects for coefficient function and matrix element. As it was reviewed in recent paper [52] the renormalization of the axial-vector current for massless quark completely suppresses the additional contribution obtained within massive approach (see section 4 of the paper).

We note that Burkhard-Cottingham sum rule is held within taking into account mass effects at the NLO level. The target mass correction of the next order ($\sim m_q^2/Q^2$) was analyzed and was shown negative in the paper [51]. However, in the case of conserved currents (see [53]) the polarized structure function g_2 with the target mass correction obeys not only Burkhard-Cottingham sum rule but and Wandzura-Wilczek relation too.

Estimating the diagrams with one-gluon radiation we have also the result for QED radiative correction to hadronic current. The calculation within the quark parton model shows that QED correction is not so large, however there are at least two arguments to be taken into account it. First, the DIS structure functions are defined for the one photon exchange approximation as an objects including only the strong interaction. It means that transferring from the cross section to the structure functions we neglect these QED

effects, so their contributions have to be included to systematic error of corresponding measurements. Second reason is that there exist some measurements where the QED correction is important. One of the example can be calculation of α_s by comparing theoretical and experimental values for the Bjorken sum rule [71]. In this case α_s is suggested to be extracted from QCD corrections to the Bjorken sum rule, which is a series over α_s, and at least five terms of the expansion are known. Simple estimation shows that the QED contribution is comparable with already fourth (or even third) term of the expansion.

There are several papers devoted to calculation of QED and electroweak corrections to the hadronic current [23–25, 31, 37, 72]. As usual methods similar ours are used for that. Positive moment here is the keeping quark mass non-zero. From the other side there are some effects which are not considered within the QED calculations: taking into account the confiment effect in integration of soft region, consideration of the quarks as non-free particles. Thus the methods (see for example [49]) developed for careful treatment of the QCD effects should be applied for the analysis of photon emission from the hadronic current. However, probably the best way to take into account the photon radiative correction to the hadronic current is further generalization of OPE technique for including of the QED effects.

3 Corrections to the lepton current in other processes

3.1 Diffractive vector meson electroproduction and code DIFFRAD

The measurement of the cross section of the exclusive vector meson electroproduction

$$e(k_1) + p(p) \longrightarrow e'(k_2) + \vec{v}(p_h) + p(p_2), \tag{94}$$

can provide information on the hadronic component of the photon and on nature of diffraction. During several years the diffractive production of the vector meson has been the subject of the muonproduction [73–75] and electroproduction [76–78] experiments. Data analysis of these experiments is considerably affected by the QED radiative effects. At practice RC to the processes of electroproduction are taken into account using codes originally developed for the inclusive case (see ref. [79], for example).

The purpose of this subsection is to present the electromagnetic correction to experimentally observed cross sections that was calculate by Bardin-Shumeiko approach in ref. [16].

We consider RC to three and four dimensional cross sections $\sigma = d\sigma/dxdydtd\phi_h$ and $\bar{\sigma} = d\sigma/dxdydt$. They are related as

$$\bar{\sigma} = \int\limits_0^{2\pi} d\phi_h \, \sigma \; . \tag{95}$$

The four differential Born cross section can be presented in the form

$$\sigma_0 = \frac{\alpha}{4\pi^2 xy}\Big(y^2\sigma_T + 2(1 - y - \frac{1}{4}y^2\gamma^2)(\sigma_L + \sigma_T)\Big), \tag{96}$$

where x and y are usual scaling variable, σ_T and σ_L are differential cross sections of the photoproduction, $\gamma^2 = Q^2/\nu^2$ and ν is the virtual photon energy.

For the observed cross section of the vector meson electroproduction we obtain

$$\sigma_{obs} = \sigma_0 e^{\delta_{inf}}(1 + \delta_{VR} + \delta_{vac}) + \sigma_F. \tag{97}$$

As earlier the correction δ_{vac} comes from the effects of vacuum polarization by leptons and hadrons.

The contribution of the infrared finite part can be written in terms of POLRAD 2.0 notation [13, 14]:

$$\sigma_F = -\frac{\alpha^2 y}{16\pi^3}\int\limits_0^{2\pi} d\phi_k \int\limits_{\tau_{min}}^{\tau_{max}} d\tau \sum_{i=1}^{2}\sum_{j=1}^{3}\theta_{ij}\int\limits_0^{v_m}\frac{dv}{f}R^{j-2}\Big[\frac{\mathcal{F}_i}{\tilde{Q}^4} - \delta_j\frac{\mathcal{F}_i^0}{Q^4}\Big], \tag{98}$$

where $R = v/f$, $f = 1 + \tau - kp_h/kp$ and $2M\tau_{max,min} = S_x \pm \sqrt{\lambda_q}$; as usual $\delta_j = 1$ for $j = 1$ and $\delta_j = 0$ otherwise. The quantities θ_{ij} depend only on the kinematic invariants and the integration variables τ and ϕ_k. The explicit expressions for them can be found in [16]. θ-functions are kinematical ones without any integrals for unpolarized case, and only one integration are left in the case of polarization part.

The dependence on the photoproduction cross sections is included in $\mathcal{F}_i$:

$$\begin{aligned} &\mathcal{F}_1 = (S_x - R)\sigma_T^R, \quad && \mathcal{F}_2 = \frac{2\tilde{Q}^2}{S_x - R}(\sigma_T^R + \sigma_L^R), \\ &\mathcal{F}_1^0 = S_x\sigma_T, && \mathcal{F}_2 = 2x(\sigma_T + \sigma_L). \end{aligned} \tag{99}$$

The quantities $\sigma_{T,L}$ have to be calculated for Born kinematics, but $\sigma_{T,L}^R$ is calculated in terms of so called true kinematics. It means that they have to be calculated for the tilde variables instead of standard Q^2, W^2 and t which have being already defined by eq. (48).

The important point is the dependence of the results on the maximal inelasticity v_m. The inelasticity is calculated in terms of the measured momenta, so it is possible to make a cut on the maximal value of this quantity. If this cut is not applied the maximal inelasticity is defined by kinematics only. Below we give the formulae for v_m in terms of the kinematic invariants

$$4Q^2 v_m = \left(\sqrt{\lambda_q} - \sqrt{t_q^2 + 4m_v^2Q^2}\right)^2 - (S_x - 2Q^2 + t_q)^2 - 4M^2Q^2. \tag{100}$$

The FORTRAN code DIFFRAD created on the basis of the presented formulae calculates the lowest order RC to the diffractive vector meson electroproduction. The higher order effects are approximated by the procedure of exponentiation. The formulae for the cross section are given in a covariant form, so the code can be run both for the fixed target experiments and for the experiments at collider.

Below we give numerical results for RC factor

$$\eta = \frac{\bar{\sigma}_{obs}}{\bar{\sigma}_0} = \frac{\int\limits_0^{2\pi} d\phi_h \sigma_{obs}}{\int\limits_0^{2\pi} d\phi_h \sigma_0} \tag{101}$$

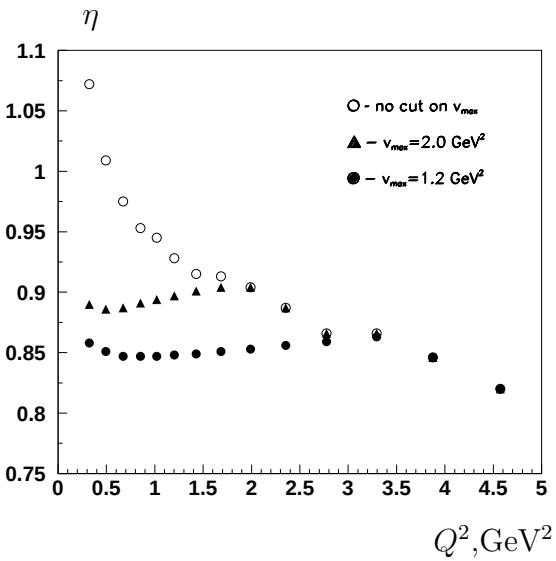

Figure 8: *RC factor under kinematic conditions of HERMES;* $\sqrt{S} = 7.9$ *GeV,* $t = -0.11$ *GeV*^{2}.

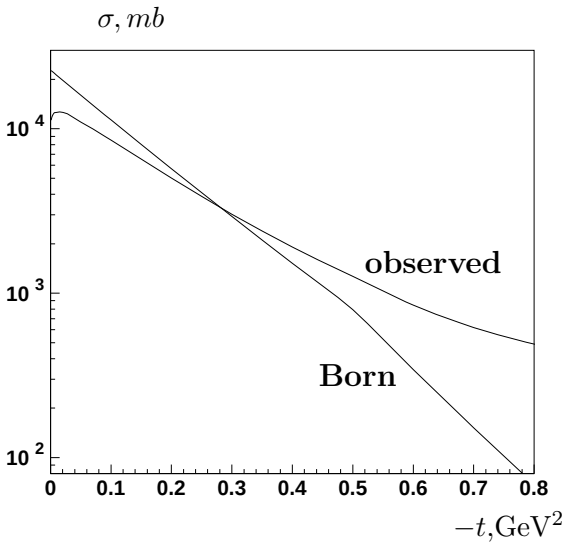

Figure 9: *Observable and Born cross sections as a function of t under kinematic conditions of HERA;* $\sqrt{s}$*=300 GeV; W=70 GeV;* Q^2*=4 GeV*^{2}.

obtained within the kinematic regions of recent HERMES and HERA experiments for exclusive $\rho(770)$ electroproduction.

The dependence on the v_m cut in the region of HERMES kinematics is analyzed in fig.8. The usage of the cut changes RC factor for small Q^2 and does not influence on RC for larger values of Q^2. In the case of the cut usage we have to define v_m as a minimum of the value of the cut and v_m given by the kinematic restrictions (100). For fixed values of $-t$ the cut influence on v_m and RC till certain value of Q^2 only.

The Q^2-dependence shown in this figure is typical for the situation when the inelasticity cut is not applied. If this cut is used then the rise of η when Q^2 goes down would be suppressed. Notice that the t-dependence is rather important too. Fig.9 illustrates this last property. η crosses unity for $-t \sim 0.25$–0.3 GeV^2 and rises with increasing $|t|$. The large positive correction in this case is a result of the large phase space for photon radiation. The cut applied to the inelasticity (or $E - p_z$) can again reduce the value of the RC factor for large $|t|$. As a consequence of the t-dependence of η, the observed slope parameter also receives large RC.

Now as application of the obtained result let us consider the process

$$e(k_1) + p(p) \to e(k_2) + p(p') + \rho(p_V), \quad \rho \to \pi^+(p_+) + \pi^-(p_-), \tag{102}$$

that can be viewed as an off-diagonal Compton scattering analytically continued in the virtuality of the photon γ^* to the vector meson mass $\gamma^* p \to Vp$ and gives access to the whole set of the corresponding helicity amplitudes.

The process (102) is analyzed experimentally by means of spin-density matrix elements. When measured, they give an indication of vector meson internal constituents motion and

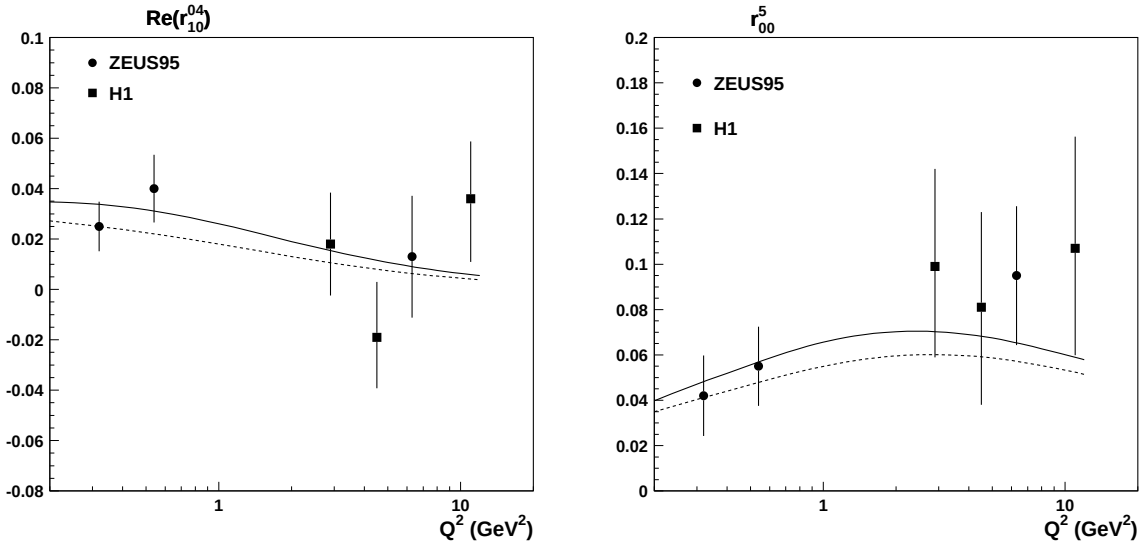

Figure 10: *The dependence of Born (dashed line) and radiative corrected (solid line) spin-density matrix elements on Q^2 under the kinematic conditions of H1/ZEUS experiments.*

its spin-angular structure. The angular distribution of unpolarized vector meson decay is parameterized by fifteen matrix elements $r_{ij}^{\alpha}, r_{ij}^{\alpha\beta}$. For a long time it was believed, that their behavior complies with the s-channel helicity conservation (SCHC) hypothesis, which means that the helicity of the virtual photon is conserved in the s-channel process $\gamma^* p \to \rho p$. In this case ten matrix elements (which corresponds to the case when photon and vector meson have different helicities) are equal to zero. But in the recent measurements r_{00}^5 has been observed to be non zero [80–82], what has been considered as an indication to SCHC violation.

The procedure of the experimental data analysis is based on the correlation of the lepton scattering, vector meson production and decay planes, which are affected by RC. Hence it is topical to look at whether the measured r_{00}^5 can, at least partly, be the result that RC coming from non-observed QED effects and real photon emission was underestimated. In any case in order to make the data processing of the corresponding experiments [80–82] to be consistent, RC should be taken into account.

As it was shown in [18] the value of the QED corrections ($\Delta r = r_{obs} - r_{Born}$) to the matrix elements are defined by the following quantity:

$$I_1 = \frac{\int\limits_0^{2\pi} d\phi_h \, \cos\phi_h \, \delta(\phi_h)}{\int\limits_0^{2\pi} d\phi_h \, (1 + \delta(\phi_h))}, \quad n = 1, ..., 4, \tag{103}$$

where $\delta(\phi_h) = \sigma_{obs}/\sigma_0 - 1$.

For the majority of the matrix elements vanishing in the SCHC limit, radiative corrections turn out to be not greater then 1%. However there are two of them, Re r_{10}^{04} and r_{00}^5, which RC appears to be substantial (see fig. 10). One can see, that corrections ΔRe r_{10}^{04} and Δr_{00}^5 may reach $\sim 20\%$.

The last result is interesting from point of view of the found SCHC violation: the radiative correction procedure reduces the observed effect.

3.2 Elastic *ep* scattering and code MASCARAD

Precise polarization measurements of nucleon form factors in electron scattering is an essential component of new-generation electron accelerators such as CEBAF [83]. This unprecedented precision requires knowledge of higher-order electromagnetic effects at a per-cent level. The purpose of this subsections is to analyze radiative corrections in elastic electron proton scattering and present computational techniques that could be used in experiments at Jefferson Lab and other electron accelerator laboratories.

The observed cross section of the process

$$e(k_1) + N(p) \longrightarrow e'(k_2) + N(p_2), \tag{104}$$

is described by one non-trivial variable, which is usually chosen to be squared of momentum transferred. There are two ways to reconstruct the variables, when both lepton and nucleon final momenta are measured. In the first way it will be denoted as $Q_l^2 = -(k_1 - k_2)^2$, and for second one it is $Q_h^2 = -(p_2 - p)^2$. It is clear that there is no difference between these definition at the Born level. However when the radiation of the lepton is only considered at the level of RC the symmetry is breaking. Here we will deal with both situations.

In the first case the structure of bremsstrahlung cross section looks like

$$\frac{d\sigma}{dQ_l^2} \sim \alpha^3 \int \frac{d^3k}{k_0} \sum \mathcal{K}\mathcal{F}^2(Q_h^2)\mathcal{A} \tag{105}$$

where $\mathcal{K}$ is a kinematic coefficient calculatable exactly in the lowest order. It depends on photon variables. $\mathcal{F}^2$ is a bilinear combination of nucleon formfactors dependent on Q_h^2 only, which is function of photon momentum. Usually only the final momenta are measured in the part of the space. It is controlled by the function of acceptance $\mathcal{A}$, which is 1 or 0 in depending whether the final particles make it in detectors or not. The integral (105) should not be analytically calculated for two reasons. The first one is dependence of formfactors on Q_h^2. We avoid to use some specific model for them. The second one is acceptance usually very complicated function of kinematic variable dependent on photon momentum.

For the second version of reconstruction of transfer momentum squared the structure of the cross section is

$$\frac{d\sigma}{dQ_h^2} \sim \alpha^3 \sum \mathcal{F}^2(Q_h^2) \int \frac{d^3k}{k_0} \mathcal{K}\mathcal{A} \tag{106}$$

In this case the squared formfactor is not dependent on photon momentum and for 4π kinematics ($\mathcal{A} = 1$) this integral can be calculated analytically. In the experimental conditions at JLab [83], both final electron and proton were detected in order to reduce background. However elastic scattering kinematics was restored by the final proton kinematics, while electron momentum was integrated over. Therefore, formalism related with Eq.(106) applies for this case.

Polarization effects are described by polarization four-vectors of the lepton (ξ) and proton (η) which can be expanded over the measured momenta k_1, p_1 and p_2. The

polarization vector of the lepton has been defined earlier by eq.(5) as well as polarization vector of the proton can be expand over four momenta of scattering particles

$$\eta \;=\; 2a_\eta k_1 + b_\eta q + c_\eta(p_1+p_2), \tag{107}$$

where the expansion coefficients defined by the different polarization states of the target.

As a result the Born cross section for the process (104) can be written in the form

$$\frac{d\sigma_0}{dQ^2} = \frac{2\pi\alpha^2}{S^2Q^4}\sum_{i=1}^{4}\theta_B^i\mathcal{F}_i, \tag{108}$$

where

$$\begin{aligned} &\theta_1^0 = 2Q^2, && \theta_3^0 = -\frac{2Q^2}{M}(Q^2a_\eta + (2S-Q^2)c_\eta),\\ &\theta_2^0 = \frac{1}{M^2}(S^2 - Q^2S - M^2Q^2), && \theta_4^0 = \frac{Q^4}{M^3}(2S-Q^2)(a_\eta - 2b_\eta). \end{aligned} \tag{109}$$

The structure functions $\mathcal{F}_i^2$ are bilinear combinations of the nucleon formfactors dependent on Q_h^2 only

$$\begin{aligned} &\mathcal{F}_1 = 4\tau_pM^2G_M^2, && \mathcal{F}_3 = -2M^2G_EG_M,\\ &\mathcal{F}_2 = 4M^2\frac{G_E^2+\tau_pG_M^2}{1+\tau_p}, && \mathcal{F}_4 = -M^2G_M\frac{G_E-G_M}{1+\tau_p}. \end{aligned} \tag{110}$$

where $\tau_p = Q^2/4M^2$.

According to [19] the cross section that takes into account radiative effects within the leptonic variables can be written as

$$d\sigma_{obs} = d\sigma_0 e^{\delta_{inf}}(1+\delta_{VR}+\delta_{vac}) + d\sigma_F. \tag{111}$$

Here the corrections δ_{inf} and δ_{vac} come from radiation of soft photons and effects of vacuum polarization. The correction δ_{VR} is an infrared-free sum of factorized parts of real and virtual photon radiation. The infrared-free contribution of bremsstrahlung process can be presented as integral over three variables: inelasticity $v = \Lambda^2 - M^2$ ($\Lambda = p + k_1 - k_2$), $\tau = kq/kp$ and angle ϕ_k between planes ($\mathbf{q}$, $\mathbf{k}$) and ($\mathbf{k_1}$, $\mathbf{k_2}$)

$$d\sigma_F \;=\; -\frac{\alpha^3}{2S^2}dQ_l^2\int_0^{v_m}dv\int_{\tau_{min}}^{\tau_{max}}\frac{d\tau}{1+\tau}\int_0^{2\pi}d\phi_k\sum_i\Big[\sum_{j=1}^{3}\mathcal{A}R^{j-2}\theta_{ij}\frac{\mathcal{F}_i}{Q_h^4} - 4F_{IR}^0\theta_i^B\frac{\mathcal{F}_i^0}{RQ_l^4}\Big], \tag{112}$$

Here $R = v/(1+\tau)$ and $\mathcal{A}$ is integrated over the ϕ acceptance function. The quantities θ_{ij} are similar to ones used in eq. (12). However there they are integrated over ϕ_k. We keep this integration because of possible dependence of acceptance function on this angle. The explicit expressions of the θ-functions in (112) are discussed in Appendix of [19].

Since within the hadronic variables the integration over the phase space of the real photon can be performed analytically, the observable cross section for this situation has more simple form

$$d\sigma_{obs} = \frac{\alpha^3}{4}\frac{dQ_h^2}{S^2Q_h^4}\sum_{i=1}^{4}[\theta_i^F + 4(\delta^{el}+\delta_{vac}^l+\delta_{vac}^h)\theta_i^0]\mathcal{F}_i + d\sigma_0. \tag{113}$$

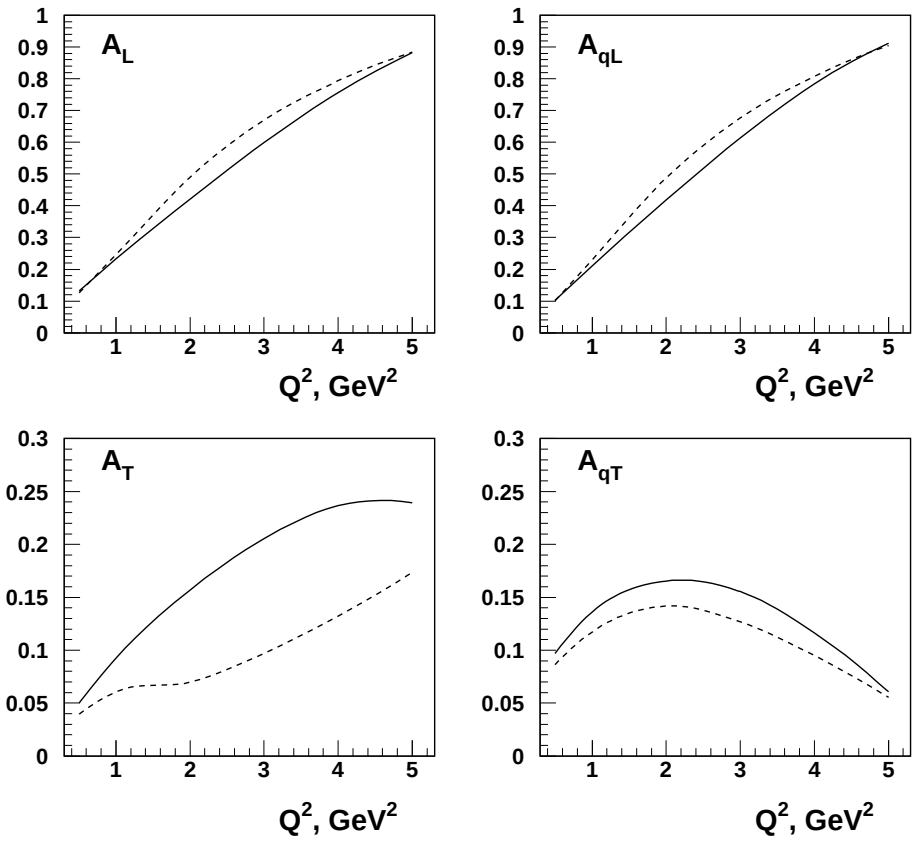

Figure 11: *Born (solid line) and observed (dashed line) asymmetries vs Q^2. No kinematic cuts on inelasticity were used. $E = 4$ GeV.*

The explicit expressions for θ_i^F and δ^{el} can be found in [20].

On the basis of formalism presented in this subsections the FORTRAN code MASCARAD developed. This code uses Monte-Carlo methods to calculate RC to the observable quantities in polarized *ep* scattering measurements.

Here we consider RC to some obsevables within two polarization measurements:

1. The initial proton is polarized and the final electron is measured to reconstruct Q^2. As a result there are four experimental situations for asymmetry definition: the target is polarized along (perpendicular) to beam or $\vec{q}$ $(q = p_2 - p)$. Corresponding polarization 4-vectors are denoted as η_L (η_T) or η_L^q (η_T^q).
2. Polarization and momentum of the final proton are measured. Two polarization states should be considered: the final proton is polarized along (η_L') and perpendicular (η_T') to $\vec{q}$.

It is natural that for the fist type of measurement we have to calculate RC within the leptonic and for the second type within hadronic variables.

Both the spin averaged and spin dependent parts of the cross section (σ^u and σ^p) can be presented as

$$\sigma_{obs}^{u,p} = (1+\delta)\sigma_0^{u,p} + \sigma_R^{u,p}. \tag{114}$$

Both the factorized correction δ and unfactorized cross section coming from bremsstrahlung process contribute to cross section.

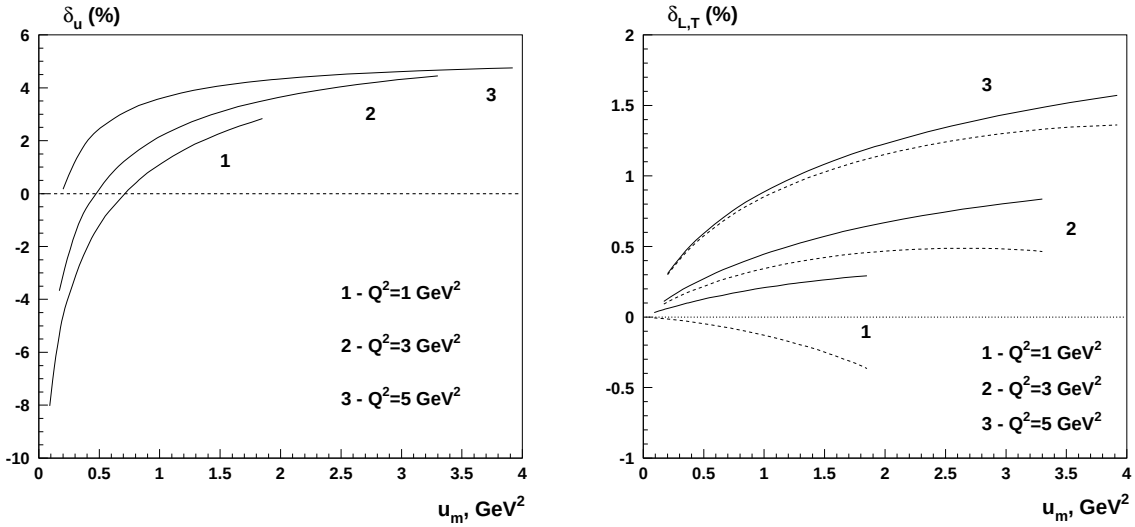

Figure 12: *Radiative corrections to the unpolarized cross section (left plot) and polarization asymmetries (right plot) defined in (46). Solid and dashed lines corresponds to longitudinal and transverse cases. S=8 GeV^2.*

Absolute and relative corrections to asymmetry can be defined as (see (114))

$$\Delta A_i = A_i - A_{i0} = \frac{(1+\delta)\sigma_0^p + \sigma_R^p}{(1+\delta)\sigma_0^u + \sigma_R^u} - \frac{\sigma_0^p}{\sigma_0^u} \tag{115}$$

$$\Delta_i = \frac{A_i - A_{i0}}{A_{i0}} = \frac{\delta_p - \delta_u}{1+\delta+\delta_u} \tag{116}$$

where index i runs over all considered cases: $i = L, T, qL, qT$; $\delta_{u,p} = \sigma_R^{u,p}/\sigma_0^{u,p}$. Here the correction δ is usually large because of contributions of leading logarithms. However it exactly canceled in numerator of expression for correction to asymmetry. That is a reason why the correction to cross section can be large while the correction to the asymmetry is relatively small.

Born and observed asymmetries are presented in fig. 11. There were no cuts for the missing mass. As a result due to unfactorizing properties hard photon contributions gives different contributions to spin averaged and spin dependent part of cross sections. For the longitudinal asymmetries $\delta_p > \delta_u$ and there are positive contributions to RC. Opposite situation with the transverse asymmetries.

For the second type of measurement let us define the relative corrections to the observables in the current experiments:

$$\delta_u = \frac{\sigma_u^{obs}}{\sigma_u^b} - 1, \qquad \delta_{L,T} = \left[\frac{\sigma_p^{obs}}{\sigma_u^{obs}} - \frac{\sigma_p^b}{\sigma_u^b}\right]\left[\frac{\sigma_p^b}{\sigma_u^b}\right]^{-1} = \frac{\sigma_u^b}{\sigma_u^{obs}}\frac{\sigma_p^{obs}}{\sigma_p^b} - 1 \tag{117}$$

The first quantity δ_u is the relative correction to the unpolarized part of cross section. The $\delta_{L,T}$ give contribution to polarization asymmetries measured by rotating the polarization states of the initial protons. The correction to the unpolarized part of cross section

is presented in fig. 12a. Its behavior is quite typical. For the very hard inelasticity cut ($u_m \ll Q^2$) the positive contribution is suppressed due to real bremsstrahlung, so there is only negative loop correction contributing to cross section. Different ending values for the curves corresponds to different kinematically allowed regions.

Conclusion

Some radiative effects in lepton scattering on polarized and unpolarized nucleons and light nuclei have been briefly reviewed. The processes of inclusive, semi-inclusive, diffractive and elastic scattering are considered. The explicit expressions for QED, electroweak and QCD lowest-order correction within Bardin-Shumeiko approach have been presented. Besides the next order correction in LO has been estimated.

Basing on the presented formulae some FORTRAN codes have been created which allow one to provide the procedure of RC of experimental data in the current and future experiments as well. More popular of them are POLRAD [14] and RADGEN [15]. The version 2.0 of FORTRAN code POLRAD provides complete RC procedure in inclusive and semi-inclusive experimental setup. Monte Carlo generator RADGEN creating from FORTRAN code POLRAD 2.0 provides event simulation with taking into account radiative effects in various experimental setup on inclusive DIS. Codes DIFFRAD and MASCARAD calculates RC in diffractive and elastic processes.

The obtained results and FORTRAN codes constructed on their basis are widely used in experimental collaborations at CERN, DESY, SLAC and TJNAF.

Acknowledgement

One of us (I. A.) thanks the US Department of Energy for support under contract DE-AC05-84ER40150.

References

[1] L.W. Mo, Y.S. Tsai//Rev. Mod. Phys. 1969. V.41. P.205.

[2] Y.S. Tsai//Preprint/SLAC. 1971. PUB - 848. P. 66.

[3] D.Yu. Bardin, N.M.Shumeiko // Nucl. Phys. 1977. V.B127. P.242.

[4] A.A. Akhundov, D.Yu. Bardin, N.M. Shumeiko // Yad. Fiz. 1977. V. 26. P. 1251.

[5] A.A. Akhundov, D.Yu. Bardin, N.M. Shumeiko // Yad. Fiz. 1986. V. 44. P. 1517.

[6] A. Akhundov, D. Bardin, L. Kalinovskaya, T. Rieman // Fortschr. Phys. 1996. V.44. P.373.

[7] A.V. Soroko, N.M. Shumeiko // Yad. Fiz. 1989. V.49. P.1348.

[8] T.V. Kukhto, N.M. Shumeiko // Yad. Fiz. 1982. V.36. P.707.

[9] I. Akushevich, D. Ryckbosch, N. Shumeiko, A. Tolkachev // J. Phys. 2000. V.G26. P.1389.

[10] A.V. Soroko, N.M. Shumeiko //Yad. Fiz. 1991. V.53. P.1015.

[11] I. Akushevich, N. Shumeiko, A. Soroko //Eur. Phys. J. 1999. V.C10. P.681.

[12] N.M. Shumeiko //Yad. Fiz. 1979. V.29. P.1571.

[13] I. Akushevich, N. Shumeiko // J. Phys. 1994. V. G20. P.513.

[14] I. Akushevich, A. Ilyichev, N. Shumeiko, A. Soroko, A. Tolkachev //Comput. Phys. Commun. 1997. V.104. P201.

[15] I.Akushevich, H.Boettcher, D.Ryckbosch //Workshop "Monte Carlo Generators for HERA Physics", Hamburg, 1998/99.

[16] I. Akushevich //Eur. Phys. J. 1999. V.C8. P.457.

[17] I. Akushevich //In *Hamburg 1998/1999, Monte Carlo generators for HERA physics* 547-553

[18] I.Akushevich, P.Kuzhir //Phys. Lett. 2000. V.B474 P. 411.

[19] A.Afanasev, I.Akushevich, N.Merenkov//hep-ph/0102086

[20] A.Afanasev, I.Akushevich, A. Ilyichev, N.Merenkov// to be published in Phys. Lett. B. hep-ph/0105328

[21] P.P.Kuzhir, N.M.Shumeiko // Yad. Fiz. 1992. V.55. P. 1958.

[22] T.V.Kukhto, N.M.Shumeiko, S.I.Timoshin // J. Phys. 1987. V.G13. P.725.

[23] D.Yu. Bardin, N.M.Shumeiko //Yad. Fiz. 1979. V.29. P.969.

[24] N.M.Shumeiko, S.I.Timoshin //J. Phys. 1991. V. G17. P. 1145.

[25] N.M.Shumeiko, S.I.Timoshin, V.A.Zykunov // Yad. Fiz. 1995. V.58. P. 2021.

[26] Adloff C, et al. //Z. Phys. 1997. V.C74. P.191.

[27] Feltesse J., Schäfer A. // "Future Physics at HERA" Proceedings of the Workshop 1995/96. P.760-776.

[28] M. Böhm, W.Hollik, H.Spiesberger //Fortschr. Phys. 1986. V.34. P.687.

[29] W. Hollik // Fortschr. Phys. 1990. V.38. P.165.

[30] I.V. Akushevich, T.V.Kukhto, F.Pacheco //J. Phys. 1992. V.G18. P.1737.

[31] D. Bardin, J. Blumlein, P. Christova, L.Kalinovskaya // Nucl. Phys. 1997. V.B506. P.295.

[32] I. Akushevich, A. Ilyichev, N. Shumeiko //J. Phys. 1998. V.G24. P.1995.

[33] D.Yu. Bardin, O.M.Fedorenko N.M.Shumeiko //Sov. J. Nucl. Phys. 1980. V.32. P.403.

[34] D.Yu. Bardin, O.M.Fedorenko, N.M.Shumeiko // J. Phys. 1981. V.G7. P.1331.

[35] D.Yu. Bardin, C. Burdik, P.Ch. Christova, T.Riemann, // Z. Phys. 1989. V.C42. P.679.

[36] M. Böhm, H.Spiesberger // Nucl. Phys. 1987. V.B294. P.1081.

[37] I. Akushevich, A. Ilyichev, N. Shumeiko //Phys. Atom. Nucl. 1995. V.58. P.1919.

[38] E.A. Kuraev, V.S. Fadin // Yad. Fiz. 1985. V.41. P.733.

[39] E.A. Kuraev, N.P. Merenkov, V.S. Fadin //Yad. Fiz. 1988. V.47. P.1593.

[40] E.A. Kuraev, N.P. Merenkov, V.S. Fadin //Yad. Fiz. 1987. V.45. P.782.

[41] I.V. Akushevich, A.V. Arbuzov, E.A. Kuraev //Phys. Lett. 1998. V.B432. P.222.

[42] I. Akushevich, E. Kuraev, B. Shaikhatdenov // Phys.Rev. 2000. V.D62. P.53016.

[43] J. Kripfganz, H.-J. Möhring, H. Spiesberger //Z. Phys. 1991. V.C49. P.501.

[44] I.Akushevich, A.Ilyichev, N.Shumeiko //Phys. Atom. Nucl. 1998. V.61. P.2154.

[45] B. Lampe, E. Reya //Phys. Rept. 2000. V.332. P.1.

[46] B. Humpert, W.L. van Neerven //Nucl. Phys. 1981. V.B184. P.498.

[47] R. Mertig, W.L. van Neerven //Z.Phys. 1993. V.C60. P.489. Erratum-ibid. 1995. V.C65. P.360.

[48] G. Altarelli, B. Lampe, P. Nason, G.Ridolfi //Phys. Lett. 1994. V.B334. P.184.

[49] O. Teryaev //Contribution to International Symp. Dubna Deutreron '95. Dubna Russia. 1995. hep-ph/9508374.

[50] O. Teryaev, O. Veretin //hep-ph/9602362.

[51] I.V. Musatov, O.V. Teryaev, A.Schäfer //Phys. Rev. 1998. V.D57. P.7041.

[52] V. Ravindran, W.L. van Neerven //Nucl. Phys. 2001. V.B605. P.517.

[53] J. Blümlein, A.Tkabladze //Nucl. Phys. 1999. V.B553. P.427.

[54] I.Akushevich, A.Ilyichev, N.Shumeiko //EPJdirect. 2001. V. C5. P.1.

[55] H. Burkhardt, B. Pietrzyk, //Phys. Lett. 1995. V.B356. P.398.

[56] G. Orlandini, M. Traini // Rep. Prog. Phys. 1991. V.54. P.257.

[57] D. Adams et al. // Phys. Lett. 1994. V.B329. P.399.

[58] D. Adams et al. // Phys. Lett. 1995 V.B357. P.248.

[59] D. Adams et al. //Phys. Lett. 1997. V.B396. P.338.

[60] D. Adams et al. // Phys. Rev. 1997. V.D56. V.5330.

[61] I. Akushevich, A. Nagaitsev//J.Phys. 1998. V.G24 P.2235.

[62] P.J. Mulders, R.D. Tangerman, //Nucl. Phys. 1996. V. B461 P.197, Erratum – ibid. 1996 V.B484 P.538.

[63] K. Ackerstaff et al., HERMES Collab. //Phys. Rev. Lett. 1998. V.58 P.5519.

[64] EMC Collab., J. Ashman et al, //Z. Phys. 1991. V.C52 P.361.

[65] HERMES. Technical design report, 1993.

[66] FERRAD 3.5 . This code was first created by J. Drees for EMC and further developed by M. Dueren.

[67] K. Ackerstaff et al. [HERMES Collaboration], //Phys. Lett. 1997. V. B404. P.383.

[68] Gagunashvili N. //Nucl. Instr. Meth. 1994. V.A343. P.606.

[69] Gagunashvili N. etal. //Nucl. Instrum. Meth. 1998. V.A412. P.146.

[70] D. Bardin, L. Kalinovskaya // DESY-97-230. Dec 1997. 54pp.

[71] J. Ellis, M. Karliner //Phys. Lett. 1995. V.B341. P.397.

[72] H. Spiesberger //Phys. Rev. 1995. V.D52. P.4936.

[73] J.J. Aubert et al. EMC Collaboration, // Phys. Lett. 1985. V.B161. P.203.

[74] M. Arneodo et al. NMC Collaboration //Nucl. Phys. 1994. V.B429. P.503.

[75] M.R. Adams et al. E665 Collaboration //Z. Phys. 1997. V.C74. P.237.

[76] S. Aid et al. H1 Collaboration //Nucl. Phys. 1996. V.B468. P. 3.

[77] M.Derrick et al. ZEUS Collaboration // Phys. Lett. 1995. V.B356. P.601.

[78] M.Tytgat, HERMES Collaboration// Proceedings of the DIS98 Workshop, Brussels, Belgium, April 1998, World Scientific.

[79] K.Kurek //DESY 96-209, 1996, hep-ph/9606240.

[80] J. Breitweg et al. ZEUS Collaboration //Eur.Phys.J. 1999. V.C6. P.603

[81] C. Adloff et al. H1 Collaboration //Eur.Phys.J. 2000. V.C13. P.371.

[82] J. Breitweg et al. ZEUS Collaboration //Eur.Phys.J. 2000. V.C12. P.393.

[83] M. K. Jones et al. Jefferson Lab Hall A Collaboration //Phys. Rev. Lett. 2000. V. 84 P.1398.